LBL-13352

Lawrence Berkeley Laboratory
UNIVERSITY OF CALIFORNIA

Engineering & Technical Services Division

A PRECISION ANALOG FIBER OPTIC TRANSMISSION SYSTEM

G. Stover
(M.S. thesis)

June 1981

Prepared for the U.S. Department of Energy under Contract W-7405-ENG-48

LBL-13352

A PRECISION ANALOG FIBER OPTIC TRANSMISSION SYSTEM

G. Stover

M.S. Thesis

Engineering and Technical Services Department
Lawrence Berkeley Laboratory
University of California
Berkeley, CA 94720

June 1981

This work was supported by the Director, Office of Energy Research, Office of High Energy and Nuclear Physics, Nuclear Science Division, of the U.S. Department of Energy under Contract No. W-7405-ENG-48.

A PRECISION ANALOG FIBER OPTIC TRANSMISSION SYSTEM

G. Stover*

I. Introduction

This article describes the design, experimental development, and construction of a DC-coupled precision analog fiber optic link. Topics to be covered include overall electrical and mechanical system parameters, basic circuit organization, modulation format, optical system design, optical receiver circuit analysis, and the experimental verification of the major design parameters.

II. System Design Parameters

The fiber optic link described in this report was designed specifically for use in the new 750-kV injector [1] presently under construction at the Heavy Ion Linear Accelerator (HILAC) facility located at Lawrence Berkeley Laboratory. The injector consists of a large metal enclosure, 10 x 16 x 13.5 feet, whose electric potential can be raised to 750 kV above earth ground. Electronic systems internal to the terminal require approximately 35 control and 86 monitor signals which are then reduced by electronic multiplexing to 6 analog and 8 digital telemetry channels. These signals must be transmitted over a non-conductive transmission medium which must withstand voltage gradients approaching 80 kV per linear foot and be immune to EMI generated by the

normal operation of the 100-kW driveshaft motor and Cockcroft-Walton high voltage generator. In addition, the system should operate reliably during any dielectric breakdown of the high voltage terminal. Given the current state of the art, the use of a fiber optic (FO) transmission system is a logical choice.

Many modern FO cables can easily withstand these gradients, and if adequate care is taken to shield the electroptic transducers, a system can be completely immune to EMI. It becomes the major task of the FO designer to create an electronic interface which satisfies the required external channel parameters and yet is insensitive to the transfer loss variations and non-linear characteristics of the FO link. The basic electronic and mechanical parameters for the analog channel are listed in Tables 1 and 2. The previously mentioned digital channel, which is a subcircuit of the analog channel, will be discussed only when its design parameters become relevant to the main topic of this report.

The primary channel requirements are defined by the system's signal source. For this particular project, most of the analog signals to be telemetered are parameters (i.e., voltage and current waveforms) generated by an array of pulsed power supplies which drive the Penning Ionization Gauge (PIG) ion source. The waveforms to be monitored have repetition rates varying from DC-36 Hz and a duty factor ranging from 5 to 40%. Typical rise times may vary from 10 to 1000 μs. A number of these waveforms may also have a superimposed fine oscillation structure $\geq$ 100 kHz generated by the PIG source. If we assume a minimum rise time of 5 μs, we have an approximated maximum bandwidth from Equation 1 of 70 kHz.

$$f_{3db} \cong .35/\ R \tag{1}$$

Adding to this the requirements of possible fine structure oscillations and the further improvement of channel phase distortion, the f_{3db} bandwidth was increased to 300 kHz. Since this particular telemetry system was designed to

accurately transmit pulse-like waveforms, it was necessary to specify leading and trailing edge overshoot and ringing characteristics. Typically, these deviations from the actual signal should be $\leq$ 1% of a 20 V peak-to-peak full-scale signal.

All of these waveforms will be displayed on control room oscilloscopes. In the future, some may be digitized and stored for computer analysis. Given the current technologies, a relative nonlinearity of .1% (deviation from a straight line) over the full dynamic range was chosen as a target parameter with the differential and total harmonic distortion (THD) specification added to provide more precise and measurable quantities.

In some special applications the monitored signal may have a pulse width of 1 minute or longer and a period between pulses of 1 day. Consequently, the system is DC-coupled with a drift specification to match the absolute accuracy specification over the anticipated temperature range. The signal-to-noise ratio was chosen to meet or exceed the full dynamic ranges of all monitored signals. The remaining specifications listed in the table are dependent on external constraints and are generally not critical to system performance.

III. Organization and Circuit Description

The final circuit design was compact enough to allow two complete telemetry channels to be contained in two single-width NIM (Nuclear Instrumentation Modules [2]) modules of 9-5/8 x 7-5/8 x 1-1/2 inches. See Figures 3, 4, and 5. To minimize cross-talk problems, both transmitter sections, and likewise both receivers, were housed in separate modules. As seen from the system diagram (Figures 1 and 2, pp. 34, 35) the complete telemetry channel is laid out in a very linear fashion.

Signals to be monitored are interfaced to the transmitter section (see schematic 1, p. 34) via a wide bandwidth, high slew rate op amp. The differential input impedance is 20 k and with matched input resistors ($\Delta R \leq 1\%$ tolerance) we can attain measured CMRR > 100 db. This factor is very crucial for the transmitter which will be in close proximity to high power rotating AC machines.

The buffer output is fed to a high frequency (5.5 MHz, max) hybridized voltage-to-frequency converter (VFC) manufactured by Device Measurements Corporation. Pot R7 controls the center frequency which was chosen to be 4.4 MHz. The VFC has a transfer function of .25 mA/MHz which, in conjunction with the buffer amplifier M2 will deviate the center frequency ±1 MHz for an input signal of ±10 volts.

The output of the VFC is a TTL pulse stream with a nominal pulse width of 100±40 ns. This waveform drives a pair of open collector buffer inverters which is followed by a grounded source VMOS LED driver. The use of a FET device noticeably improves current rise and fall times and eliminates storage effects observed in bipolar devices. The LED driver network is configured to provide a fairly constant current load to the +5 V supply to minimize switching transients. This is accomplished by diverting diode current through the FET rather than blocking its flow during the off period.

The output of the VMOS device marks the beginning of the electroptical transmission system which is comprised of a photodiode emitter, an interconnecting fiber optic cable, and a photodetector. Specific design details will be discussed more completely in the section titled Fiber Optic Link Design.

The current pulses received from the photodetector are fed to a low-noise DC-coupled, wide bandwidth current-to-voltage converter comprised of Q1, 2, and 3 (see schematic 2). The threshold detection and conversion to T^2L levels is achieved through a high-speed comparator and latching buffer M1. The recovered pulse waveform is then sent separately to a frequency-to-voltage converter (demodulator) and carrier detector circuit. The detector consists of a dual retriggerable one-shot which simultaneously turns off a front panel LED indicator and transmits an alarm to external equipment when the pulse stream has been lost for over 3 μs.

The FVC, which is adjusted by Pot R5, is set to deliver a 0 volt output for a monotonic 4.4 MHz input pulse stream. The demodulated output is recovered by a four-pole low-pass linear phase response filter whose output drives the noninverting input of dual buffered linear drivers. This configuration allows for complete source isolation between separate output loads. The amplifiers, which have continuous short circuit protection, are capable of driving 50-ohm lines ±10 volts. DC offset adjustment of both amplifiers is provided by front panel resistor R6.

Power for circuits in the transmitter and receiver modules is derived from ±24 V, +12 V supplies in the NIM bin which is regulated down to ±15 V and +5 V by regulators located in the NIM modules.

IV. Circuit Design Considerations

A. Modulation Schemes

When designing an analog fiber optic link which requires a reasonable DC stability, the first design consideration is the type of modulation to be used.

Most digital fiber optic systems employ a straightforward form of intensity modulation. This method is easily adaptable to fairly linear, wide bandwidth amplitude modulation schemes. Unfortunately, the transmission prop- erties of the electroptic transducers and to a lesser degree the fiber optic cable itself are notably sensitive to temperature variations. Though there are optical feedback schemes [3] to compensate for these problems, the simpler solution employs the use of an amplitude independent modulation technique. Of these, the most popular include frequency modulation (FM), phase modulation (PM), and several types of pulse modulation.

In the design of this particular system, physical size along with the electrical requirements was an important consideration. It was desired to have at least two analog channels per single-width NIM module which required that the IC parts count be kept to a minimum. This aspect directed my search for a modulation scheme which was modular in nature and required very few external discrete parts. Three methods were considered.

The first was a high-frequency phase-locked loop (PLL) IC (NE560) manufactured by Signetics. This design employed the VCO section of the IC as the modulator, and the complete PLL loop as a tracking demodulator. A system employing this technique had fallen short of the desired specifications. The major problem lies in the type of VCO employed in high frequency (> 1 MHz) PPL IC's. In most cases, these oscillators are simply RC multivibrators using an emitter-coupled configuration for speed. These circuits display considerable sensitivity of center frequency to temperature, typically 600 to 3000 ppm/°C, which seriously degrades the desired DC characteristics [4]. Added to this is the fairly high amount of oscillator phase jitter which contributes to the lowered signal-to-noise ratios. For wide bandwidth DC-coupled systems this circuit is unacceptable.

A simple form of Pulse Code Modulation (PCM) had been considered using a matched pair of A/D-D/A modules. This concept is workable but complex design problems exist. If one desires a 300 kHz bandwidth and samples at three times the Nyquist criterion, we have a 900 kHz sample rate. In order to obtain an acceptable dynamic range, 10 bits of resolution is required. Adding 2 stop bits per word, we have 900 kHz x 12 bits = 10.8 Mbs data rate. Cost-effective digital fiber optic links were available that could transmit this data rate, but circuit complexity and the very limited availability of cheap 10 bit A/D converters with conversion times under 1 μs ruled against this option.

A third design choice which proved to be far superior to either of the above, and was subsequently employed in this design, was a matched VFC/FVC module pair. This is a pulse modulation scheme where the carrier is a series of periodic pulses. Information is conveyed by modulating the frequency of the pulse stream and is aptly termed pulse-frequency modulation (PFM). Since the variation in the pulse frequency is proportional to the modulating signal at periodically spaced sampling times, the sampling scheme is defined as "uniform." The expression for the spectra of a uniform PFM signal is given by Equation 2 [5].

$$p_m(t) = \underbrace{\frac{A\omega_r\tau}{2\pi} + A\left(\frac{\Delta\omega}{2\pi}\right) \sin\frac{[\omega_m(\tau/2)]}{\omega_m(\tau/2)} \cos[\omega_m t + \phi - (\omega_m\tau/2)]}_{\text{DC component}}$$

$$+ A\omega_r\tau/\pi \sum_{k=1}^{\infty} \underbrace{\left(J_o(k\beta) \sin\frac{[k\omega_r(\tau/2)]}{k\omega_r(\tau/2)} \cos(k\omega_r t) + \right.}_{\text{carrier}} \qquad (2)$$

$$\sum_{n=1}^{\infty} J_n(k\beta \times \ldots .)\Big)$$

sidebands.

The zero or the DC component of the pulse spectrum has a sideband of the modulating frequency. Modulation can therefore be recovered by means of a low-pass filter, and there will be no harmonic distortion as there are no harmonic terms in the zero-order pulse spectrum. The only form of distortion which can occur comes from the lower sidebands of harmonics of the pulse-repetition frequency which penetrates into the demodulating filter pass band.

Figure 6 shows the observed output spectrum of the VFC pulse train modulated by a 350 kHz sine wave. For this particular test, the carrier frequency was 4.5 MHz. Ignoring the extra harmonic components generated by distortion in the signal generator (.7, 1.05, and 1.4 MHz), we can see a separation between the modulation frequency and lower harmonic sidebands of over 1.5 MHz. A reasonably sharp cut-off filter would adequately attentuate all unwanted components.

B. Demodulation Filter

In the design of filters where the linearity of the phase characteristic inside the pass band is important, we need a response that approximates a Gaussian characteristic curve. This particular response provides minimal delay distortion of the pulse waveform, and additionally has a frequency characteristic with a fairly steep roll-off of 40 to 60 db per decade. A class of linear phase circuits that approximates these requirements are known as maximally flat time delay filters, which have transfer functions very similar to the modified Bessel function response [6]. The frequency curves for these

filters are shown in Figures 7 and 8. The four pole response was chosen for minimal parts count, adequate roll-off, and reasonable approximation to a Gaussian characteristic (Figure 8 for n = 4). The filter was implemented in a passive design which obviated the need for the use of expensive high slew rate operational amplifiers that active filter designs would have required.

Figure 9 shows the filter pulse response with a passive load. A rough measurement of the overshoot deviation shows a good agreement with the 1% specification. The effectiveness of the filter can be observed in Figures 10 and 11. The hash-like noise observed in the upper waveform is due to carrier and sideband harmonic feed-through from the demodulator. The lower traces are obtained after filtering.

Up to this point, we have assumed a black-box approach to the converters. In order to comprehend their wideband response and very good linearity, I will briefly discuss their internal circuit functions.

C. VFC, FVC Circuit Description

The voltage-to-frequency converter used in this design is a precision relaxation oscillator that generates an output frequency linearly proportional to the input voltage. As seen in Figure 12, the circuit contains a very stable capacitor (C1) which is alternately switched between the precision voltage reference and the summing node of the integrator amplifier. Generally speaking, the circuit is a feedback loop that keeps the total charge transfer at the integrator node constant. When the charging ramp crosses the upper threshold of the Schmitt trigger, the Schmitt fires the one-shot: 1) generating an output pulse of short, fixed duration, and 2) causing the charge dispenser to dump a fixed charge ($Q = C1 \cdot V_{ref}$) into the summing node of the integrator which

generates the restoration phase of the relaxation oscillator. The restoration phase is of a fixed, short duration determined by the one shot, but the charging phase duration, with C1 effectively out of the circuit, varies directly with the input current, causing the output pulse frequency to vary in an inverse proportion. If the circuit has a very stable Schmidt threshold voltage and a reasonably high loop gain, the linearity of the module is inherent. Problems of frequency drift with temperature would be largely dependent on internal reference, capacitor C1, and Schmidt threshold stabilities. Most high frequency VFC's exhibit moderately good temperature characteristics.

The frequency-to-voltage converter is an open loop version of the VFC module as shown in Figure 13. The input pulse train triggers a one-shot flip-flop which toggles the charge dispenser switches. Current pulses delivered to the integrator are summed together to generate the demodulated output. Other than nonlinearities in the charge dispenser, this receiver is inherently linear and reasonably stable. From Table 3 of the DMC system specifications, we observe an accuracy of .1% and a temperature coefficient of 100 ppm/°C. This concludes the discussion of the interface circuitry. We now turn our attention to the fiber optic transmission medium.

V. Fiber Optic Transmission System

A. System Components

The basic electro-optic system consists of a pigtailed emitter and detector (TXED 489, 455) manufactured by Texas Instruments Inc., the transmission cable (PFX S120-T30) by E. I. Dupont and Co., and the fiber cable connectors by AMP, Inc. Specifications for the cables and transducers are listed in Tables 4, 5,

6, 7, and 8. The emitter is a very small area GaAlAs infrared-emitting diode with a peak emission wave length of 790 nm. The p-n junction is formed by multiple liquid-phase epitaxial layers for maximum quantum efficiency. The diode is contained in an epoxy-filled dual-in-line plastic package which is mounted in a socket on the PC board. A large-diameter plastic core (400 μm) fiber optic cable is positioned directly over the emitter chip for maximum coupling of light into the fiber. This 25 cm plastic cable "pigtail" is coupled to the main transmission cable via an AMP bulkhead splice mounted at the back of the NIM module. Optical output power at the end of the pigtail is greater than 200 μW for 100 mA of forward current. The radiant light rise time is ~8 ns.

Light from the emitter, having passed through the main transmission cable, is transmitted through a second bulkhead splice to a identically packaged detector assembly. The detector transducer is a silicon p-i-n photodiode employing high-resistivity silicon for high responsivity and low capacitance at low reverse voltage. The diode is fully depleted at 5 volts and has a rise time of 8 ns. At 25 volts the rise time drops to only 3 ns. This detector also features a built-in reference diode for dark-current circuit compensation at high temperatures. The radiant responsivity (R), referenced to the radiant power incident on the input end of the pigtail, is typically .3 A/W which is ~60% of the nominal .5 A/W observed for most silicon photodetectors free from aperture constraints. The coupling of this photodetector to the emitter requires a compatible optical transmission cable and connector system.

The cable chosen was a medium loss, less than 40 db/km, pure-silica core fiber with a hard plastic cladding. This is a step index fiber, $n_{core} < n_{clad}$, with a strong absorption peak at 950 nm largely due to OH^- ions in the silica.

The photoemitter peak emission wavelength is located well within the region of the lowest attenuation characteristic of the cable. The cable has a fairly large numerical aperture (.42), a figure of light acceptance angle, a low dispersive rise time characteristic (8 ns/.2 km), and reasonable core concentricity ($\leq$ 18%). Beyond its optical characteristics, it is fairly cheap ($2 per m) and very rugged, which even the specifications do not fully convey. One of the key design requirements was compatibility with an inexpensive field-installable connector. The hard plastic cladding of this particular cable makes a very good bond with the epoxy glue used to hold the connector ferrule to the fiber.

The process of connector installation is fairly simple. After the epoxy has cured, which may take as little as 5 minutes, the fiber and ferrule tip are hand polished in a four-step grinding process.

B. Transmission Parameters

As with any basic transmission system, there are two basic design parameters to be considered: channel bandwidth and the minimum acceptable optical power into the receiver. Even though loss is usually the most critical, the highly touted excess bandwidth of fiber optic cables doesn't always follow for medium-loss cables. Bandwidth limitations in fiber optic cables are the result of material and modal dispersion. Both of these parameters relate to the velocity of flux transmission in the core. For broad-spectrum noncoherent sources, these effects are magnified. In combination with the cable, we have rise time considerations of the emitter, detector, and receiver.

The proposed modulation scheme for the analog transmission system requires a maximum bandwidth of 6 MHz, which also includes the 10 Mb/s data rate

required by the digital systems. Allowing for some design margin, a design frequency of 10 MHz was chosen. If we assume that the impulse response of a fiber optic link can be approximated by a Gaussian curve in the time domain [7], we can take the Fourier transform to arrive at an approximate optical or electrical bandwidth as a function of the rise time. See Equations 3 and 4.

$$f(-3 \text{ db optical}) = 0.188/t_\sigma \tag{3}$$

$$f(-3 \text{ db elect.}) = 0.133/t_\sigma \tag{4}$$

t_σ in these equations is 1/2 the standard deviation width of a Gaussian pulse. Equation 5 gives the relationship between t_σ and the 10-90% pulse rise time.

$$T_{10-90\%} = 1.69\ t_\sigma \tag{5}$$

By knowing the bandwidth, it is possible to calculate the rise time and maximum signal rate possible over the fiber system.

When a pulse is transmitted through an optical system, each component can act on this pulse to change its rise time. Assuming a Gaussian case, the rms pulse width of the various components can contribute to the overall final pulse width by Equation 6.

$$t_\sigma^{tot} = (t_{\sigma_1}^2 + t_{\sigma_2}^2 + t_{\sigma_3}^2)^{1/2} \tag{6}$$

For the following values:

$$t_{\sigma_1}(\text{cable}) = 8 \text{ ns}/.2 \text{ km} = 4 \text{ ns}$$

$$t_{\sigma_2}(\text{LED}) = 8 \text{ ns}/1.69 = 4.7 \text{ ns}$$

$$t_{\sigma_3}(DET) = 4 \text{ ns}/1.69 = 2.4 \text{ ns}$$

we have:

$$f(-3 \text{ db elect.}) = .133/6.62 \text{ ns} = 20.1 \text{ MHz} \quad (7)$$

$$T_{10-90} = 1.69 \cdot 6.62 \text{ ns} = 11.2 \text{ ns} \quad (8)$$

To obtain the data rate (DR) one can use the common criterion that T_{10-90} is no more than 70% of the bit width for a NRZ code. This gives:

$$DR(NRZ) = 1/t_{bit} = .7/T_{10-90} = .7/11.2 \text{ ns} = 62.5 \text{ Mb/s}.$$

From these calculations we have a fairly reasonable bandwidth and data rate margin. It will be shown in later experimental results that the contribution of comparable transmitter and receiver rise times will narrow this margin considerably.

The second design parameter is the minimum optical power requirements for the fiber optic receiver. The power level at the receiver must be high enough that the signal-to-noise ratio (SNR) insures an adequately low probability of error (P_e) in the threshold detection of the received pulse. Otherwise, the bit error rate would be unacceptable for digital systems and the ϕ noise too high for the analog system. Several receiver designs were prototyped and evaluated. The final version, which was developed by co-designer William Hearn, is a creative variation on a well-known low noise transimpedance amplifier.

The circuit consists of a matched pair differential input stage (Q3) with a FET (Q1) in cascode to reduce miller effect capacitance. The amplified output of Q1 is fed through emitter follower Q2 and level shifted via zener Z1. The closed loop gain of the amplifier is controlled by a shunt, shunt feedback network consisting of resistor and capacitor R2, C2. In order to determine

the minimum optical power requirement, we must calculate the equivalent input rms noise current of the amplifier. Considering the case of shunt feedback at the input and adequate open loop gain $A_{OL} \simeq 120$ (Appendix I), we can write the equivalent input noise current as [4]:

$$\overline{i_i^2} = \overline{i_{1a}^2} + \frac{2\,\overline{V_{ia}}^2}{R_f^2} + 4\,kT\,\frac{1}{R_f}\,\Delta f. \tag{9}$$

This equation represents the input noise of the basic amplifier together with a term representing thermal noise in the feedback resistor. The "2" in the second term comes from the summation of noise sources in the differential pair [4]. The sources of noise for the input transistor consists mainly of shot and thermal noise with flicker and burst noise being excluded due to the very high current gain of the input transistors ($\beta \geq 300$). Calculating the equivalent input noise sources of the device and external components, we have:

$$\frac{i_n^2}{\Delta f} = 2qI_B + 4\,kT/R_f \tag{10}$$

and

$$\frac{i_n^2}{\Delta f} = 2\,kT\,[\frac{1}{g_m}]\,(2\pi\,fC_T)^2 + 4\,kT(r_g + r_b')\,(2\pi\,fC_d)^2 \tag{11}$$

We find that the noise sources can be divided into a "white" and "f^2" noise. The "white" noise component is comprised of input transistor base current shot noise and thermal noise from the feedback resistor. The "f^2" noise arises from the various noise voltages in the preamp circuit interacting with reactive

components of the photodiode and input transistors. The presence of the "f^2" noise dictates that the amplifier must have at least two poles in the high-frequency roll-off characteristic to insure that the total noise will be bounded. As with most multistage active circuits, there are at least two dominant and generally several more minor high frequency poles in the overall transfer function. In this particular case, feedback resistance R2 and the total input capacitance C_T generate the first, and Q1's drain capacitance C_d and it's load resistance develop the second. The equivalent white noise bandwidth of a two pole network can then be approximated by Equation 12 [10].

$$f_w = Nf_1 \tag{12}$$

where $N \cong \tan^{-1}\left[\dfrac{1/a_1}{\pi/2 - \tan^{-1} 2a_1/\pi}\right]$

and $a_1 = f_1/f_2$.

Similarly, the noise bandwidth of a two pole network for "f^2" noise is:

$$f_{f^2} = M f_1 \tag{13}$$

where $M = \left[\dfrac{\pi}{2a_1} - \tan^{-1}\dfrac{1}{a_1}\right]$.

The complete equation for the equivalent input noise is:

$$i_i = (2q I_B + \frac{4 kT}{R_f})fw + [4 kT [\frac{1}{g_m}] (2\pi f_1 C_T)^2 + 8 kT (r_b' + r_s) (2\pi f_1 C_D)^2]f_{f^2} \tag{14}$$

where

R_f = feedback resistor;

r_b' = base resistance of transistor;

r_s = series resistance of photodiode;

g_m = transconductance of Q1A;

C_T = total capacitance of preamp input;

C_D = capacitance of photodiode.

Theoretical computations, performed in Appendix I, give an input rms noise current of 12.6 na. This translates to a minimum input power, for a signal-to-noise ratio of unity, of 42 nanowatts. For the digital system, a BER of 10^{-9} or better, assuming normal Gaussian non-signal dependent noise, requires a minimum S/N of 16 db [8, 9] which implies a minimum input power of .265 μW. A somewhat harder number to arrive at was the minimum input power to insure an acceptable ϕ jitter in the pulse frequency system.

Pulse frequency modulation schemes are mainly sensitive to ϕ noise. The sensitivity of the converters is not specified, and requires the detailed analysis of the internal circuitry, which was not available from the manufacturer. Bench tests of the converters revealed that ~2 ns of ϕ jitter on the leading edge of the modulation pulse caused noticeable signal degradation. From this empirical observation, it was decided to set the minimum input power for analog and digital systems to 1 μW.

Once the minimum input power requirements are obtained, we can calculate the entire optical system loss to determine the emitter power requirements and permissible cable configurations. A theoretical calculation was performed in Appendix II using the TI emitter and detector with 100 meters of PFX S120-T30 fiber cable and one extra cable splice beyond the normal requirements of two,

one at each bulkhead. The minimum worst case output power was found to be 4.57 μW which gives a minimum power margin of 4.1 db.

VI. Results and Conclusions

A. Optical System

Power margin tests were conducted on the bench and after system installation. Various emitter power levels, cable types, and cable combinations were tested. All optical power measurements were made with the 22XL optical photometer manufactured by Photodyne, Inc. See Table 9 for specifications. The meter was calibrated, within 1%, at an optical center frequency of 800 nm.

From Appendix III, we see that the maximum and average experimental losses were less than predicted by theory with two exceptions. In the case of cable attenuation measurements, the method of accurately determining cable loss requires a well-collimated monochromatic source, usually a laser, which was not available at the time these specifications were being verified. As a substitute, a standard LED source was used with an estimated accuracy of ±25%.

The second noticeable deviation from theory was the splice loss between two identical S120 cables. The high value (8 db) would indicate a very serious problem in estimating splice losses in any optical system using AMP plastic connectors. Fortunately, the problems leading to this loss factor were identified and corrected.

The first was the accidental switch of two of the four very fine grit polishing papers. The reversal, which left the fiber surface much rougher than expected, caused an excess average loss of 2 db. The second problem, which seemed to cause an extra 3 db of loss, was due to axial misalignment. This

arose from a combination of excessive core concentricity deviation and sloppy bore diameter tolerance in the connector ferrule. Early versions of the plastic connector manufactured by AMP were not meeting their specifications. In both cases to date, the problems have been ameliorated by the manufacturers to the point that the mean splice loss has dropped to 2.5±.5 db. If a designer requires lower losses or tighter specifications, he should consider the more expensive metal connectors now on the market.

The total systems rise time from the emitter, through 6 m of S120 cable, the detector, and finally the receiver output (node 1 on schematic 2) can be calculated from Figures 14 and 15. $T_{R/F}$ (10-90%) is ~25 ns. This gives an f(3db elect.) of 9.0 MHz and a DR(NRZ) of 28 Mb/s. Though this is still well above the 6 MHz bandwidth required, it's a factor of 2 lower than estimated when considering the optical system alone. The chief factor in the lowered response times was the parasitic capacities of the optical receiver. The feedback capacitor C2, which stabilizes the receiver, could have been lower if the second dominant pole ($_{2}$, = C_{drain} + C_{trace} x R_L) was higher in frequency. This circuit was fairly layout sensitive. With improved layout designs or IC implementation, this circuit can be pushed to 30 MHz [10]. Unfortunately, increased bandwidth would generate increased input noise.

Accurate measurement of the receiver input noise current was rather limited due to the instrumentation available. Two methods were employed. The first measurement was the output noise of the amplifier with a true rms voltmeter (HP 3400 A) and no optical input signal. Calculations made in Appendix IV give a measured value of 7.8 na or 4.2 db below the theoretical result. Given the assumptions made in the calculations, this shows fairly good agreement between theory and experiment.

The second noise measurement was made under a dynamic situation. A digital 5 MHz pseudo-random sequence (32,767-bits long) was transmitted through the fiber link and checked for bit errors at selected optical power levels. Code generation and error detection were implemented by a Tautron PCM-TDM digital transmission set PTS-107. The transmission rates and counting period were set for a BER probability of $\sim 10^{-3}$. Measurements and calculations for a two-level Gaussian noise function, see Appendix V, give an equivalent input noise current of 30 na. This is ~11.7 db above the static noise measurement of 7.8 na. The increased noise level is most likely due to the switching transients generated by the high speed comparator. If lower dynamic noise levels were required, the receiver could be shielded more completely from the comparator. The dynamic input noise level raises the minimum theoretical input optical power level to .631 μW. If we include a 3 db power margin for phase jitter, this gives 1.26 μW which is in very close agreement with the minimum optical power (1 μW) chosen after bench test observations.

The actual fiber system link requirements were much less demanding than the theoretical design. To date, there are 6 analog and 20 digital links, all of lengths less than 50 meters and no additional intervening cable splices. Average power levels are typically 7.6 μW. Having characterized the optical link, we now discuss the analog channel parameters.

B. Analog Channel System Parameters

One of the more unpredictable but very important parameters was the system signal-to-noise ratio and its relationship to optical power levels. The noise floor, at the output of the complete system, was measured with an HP 3400A. The maximum output signal was defined as a 20 V p-p sine wave. The measured

signal-to-noise ratio (Appendix V) with a 46 meter cable was 71.1 db. A 1 db decrease in the S/N ratio was observed at a measured optical input power of 1.95 μW and a 3 db signal degradation occurred at a 1.23 μW. This gives minimum power requirement of 2 μW or a noise margin above the theoretical worst case loss of 3.6 db. For this configuration, two 50-meter links with a splice in-between, this system would be a little marginal. Fortunately, 3 to 4 db could be squeezed out of the emitter if required.

The bandwidth was measured by swept frequency technique with a f_{3b} point of 318 kHz. Of greater relevance was output filter pulse response to a fast rising waveform, Figure 16. Even though it's band limited, the pulse shows no overshoot or ringing, and falls well within the 1% of the ideal requirement.

The linearity was divided into several characteristic measurements. The full dynamic range of the system can bee seen in Figure 17. If we invert the output waveform and add it to the input, we get the difference signal shown in Figure 18. Except for a mismatch in channel gains, the gross non-linearity n ever exceeds 20 MV from end to end, which easily meets the .1% criterion. At typical signal levels (5 p-p) the total harmonic and intermodulation distortion was calculated (from Figures 19 and 20, and Appendix VI) to be .2% and .67% which approaches the quality of high fidelity in audio applications. It was noticed that THD and IMD were relatively sensitive to the threshold level adjustment and optical power level. If the system requires minimum distortion, the threshold level in the transimpedance amplifier should be set with a distortion analyzer connected to the output buffer amplifier.

The final parameter is system temperature drift. It was calculated to be ~80 mV for $\Delta 10^{\circ}C$. Bench tests gave a value of ~100 mV for $\Delta 10^{\circ}C$.

C. Conclusion

This report has described the design and reported the measured performance of an economic and compact precision analog fiber optic link. Basic problems in optical link design, receiver design, and modulation formats were considered. The complete system has been constructed, installed, and operated in the Third Injector system. Except for a few initial adjustments and design changes, the system has operated trouble-free for the last several months.

Permissions

1. Table 3, and Figures 12 and 13, reproduced with permission of Dynamic Measurements Corp., Winchester, MA, January 2, 1982.
2. Tables 4,5,6, & 7 c , 1980, reproduced with permission of Texas Instruments, Dallas, TX, January 11, 1982.
3. Table 8, c , December 1980, reproduced with permission of E.I. DuPont de Nemours, Inc., Wilmington, DE, December 8, 1981.
4. Table 9 c , 1979, reproduced with permission of Photodyne, Inc., Newbury Park, CA, December 8, 1981.
5. Figures 7 and 8, c , 1975, reproduced with permission of ITT, Howard W. Sands Co., Inc., Indianapolis, IN, December 8, 1981.

References

* This work was supported by the Director, Office of Energy Research, Office of High Energy and Nuclear Physics, Nuclear Science Division, U.S. Dept. of Energy under Contract No. W-7405-ENG-48.

1. High Intensity Uranium Beams National Facility from the SuperHILAC and BEVALAC, Technical Description, Lawrence Berkeley Laboratory, Feb. 1979, PUB-5023.

2. Standard Nuclear Instrument Modules, Engineering Report, AEC NIM Committee, July 1974, TID-20893 (Rev. 4).

3. Jozef Straus, Linearized Transmitters for Analog Fiber Links, Laser Focus, p. 54, Oct. 1978.

4. Paul R. Gray, Robert G. Meyer, Analysis and Design of Analog Integrated Circuits, John E. Wiley and Sons, 1977.

5. Philip E. Panter, Modulation, Noise, and Spectral Analysis, McGraw-Hill, 1965.

6. Reference Data for Radio Engineers, Howard W. Saurs and Co., Inc., 6th ed., 1975.

7. J. L. McNaughton, R. L. Ohlhaber, Signal Transfer Characteristics of Fiber Optic Cable, Belden Corp.

8. John F. Midwinter, Optical Fibers for Transmission, John Wiley and Sons, 1979.

9. Bell Telephone Laboratories, Transmission Systems for Communications, Bell Telephone, Feb. 1970.

10. J. R. Biard, Optoelectronic Aspects of Avionic Systems, Tech. Report AFAL-TR-73-164, April 1973.

Table 1
Electrical System Specifications

Bandwidth	DC - 300 kHz
Overshoot and ringing (system)	$\leq$ 1% of full scale
Differential nonlinearity	$\leq$ 50 mV from ideal
Nonlinearity	$\leq$ .1% of full scale
Distortion (large signal, 5 V p-p)	$\leq$ .1% THD
Absolute accuracy	$\leq$ 1% of full scale
S/N (max signal/no signal)	$\geq$ 60 db
Drift (±10°C from nominal)	$\leq$ .5% of full scale
Z_{in} (differential)	= 20 k
Z_{out}	= 100
Max signal swing	±10 V
Individual module power requirements	1/12 of standard NIM power supply (2)
DC offset	±5 V adjustable

Table 2

Mechanical System Specifications

Transmission distance	$\leq$ 50 meters
Interconnections	1 splice (optional)
Package size	2 channels single-width NIM module (2)
Shielding	RF-tight

SYSTEM 5500 OPERATING SPECIFICATIONS

Typical and nominal at +25°C unless otherwise noted

SYSTEM PARAMETERS

Operating Voltage Range①	± 10 Volts
Input Impedance	7KΩ
Accuracy (1.5 to 5.5MHz)	Within ± 0.1% (max.) of operating span
Stability of Accuracy	
T.C.	± 100 ppm/°C of span, max.
Drift (per day)	± 150 ppm of span, max.
Drift (per month)	± 300 ppm of span, max.
PSRR	± 0.002%/%

①With input/output scaling to place the frequency span within the 1.5 to 5.5MHz range.

5501 INPUT MODULE (VFC)

Operating Voltage Range	-10μV to -10V (neg)
Overrange	10%, min.
Impedance	7KΩ
Maximum Input Voltage	± Vcc
Transfer Characteristic f_{out} =	5MHz (Ein/10V ± Foffset ②)
Output Pulse	100ns ± 40ns
Levels 1 (high)	+4V ± 0.5V
Levels 0 (low)	<0.4V @ 16mA sink current
Fanout	10 TTL loads
Capacitor Load Capability	50pF for rated performance
Short Circuit Protection (to ground)	Indefinite short without damage
Response (settling time)	1 to 2 cycles of new frequency +2μs
Overload Recovery	12 cycles of new frequency
Supply Voltage (Vcc)	±15V ± 5% (±13V to ±18V abs. limit)
Power Drain	(+49, -21)mA typ; (+53, -23)mA max.
PSRR	± 0.002%/% max.
Temperature	
Operating	0°C to +70°C
Derated 50% TC, Linearity & Fanout	-25°C to +85°C
Storage	-25°C to +95°C

②Foffset = -4MHz x Iin (mA) (where Iin is applied to Offset Adjust pin)

5502 OUTPUT MODULE (FVC)

Input	
Frequency Range	0 to 5MHz plus 10% overrange
Impedance	One TTL load
Timing	Positive pulse; 30ns wide, min.
Output	
Voltage Range	0 to -10 Volts plus 10% overrange
Offset Range	±10 Volts (±1.4mA at I_{in} pin provides approx. ± 10 Volts offset)
Transfer Characteristic	$V_{out} = -10V\ (\frac{F_{in}}{5MHz}) \pm V_{offset}$
Power Requirements	
Voltage	±15V ± 5%
Current	(+53, -23)mA, max.
PSRR	±.002%/%, max.
Temperature	
Operating	0°C to +70°C
Storage	-25°C to +85°C

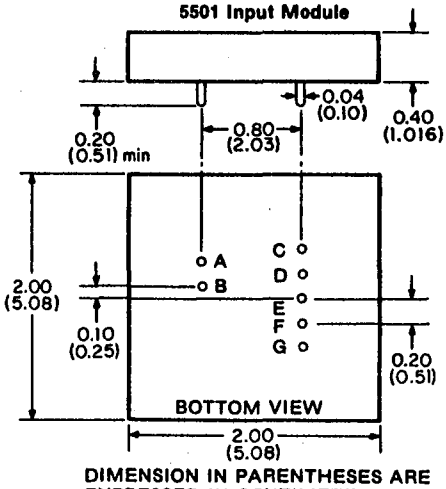

DIMENSION IN PARENTHESES ARE EXPRESSED IN CENTIMETERS.

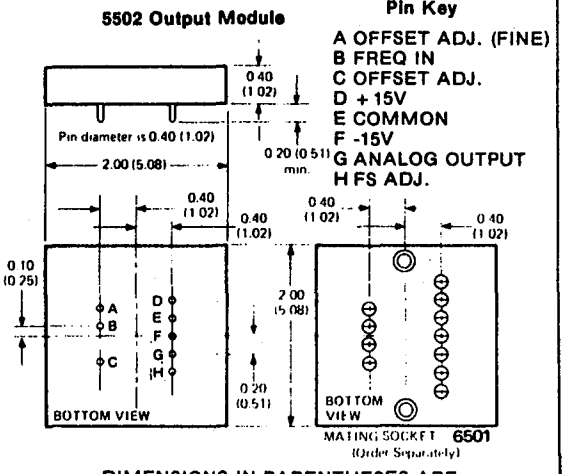

DIMENSIONS IN PARENTHESES ARE EXPRESSED IN CENTIMETERS.

SERIES TXES478 THRU TXES483 Table 4
FIBER-OPTIC GALLIUM ALUMINUM ARSENIDE SOURCE ASSEMBLIES

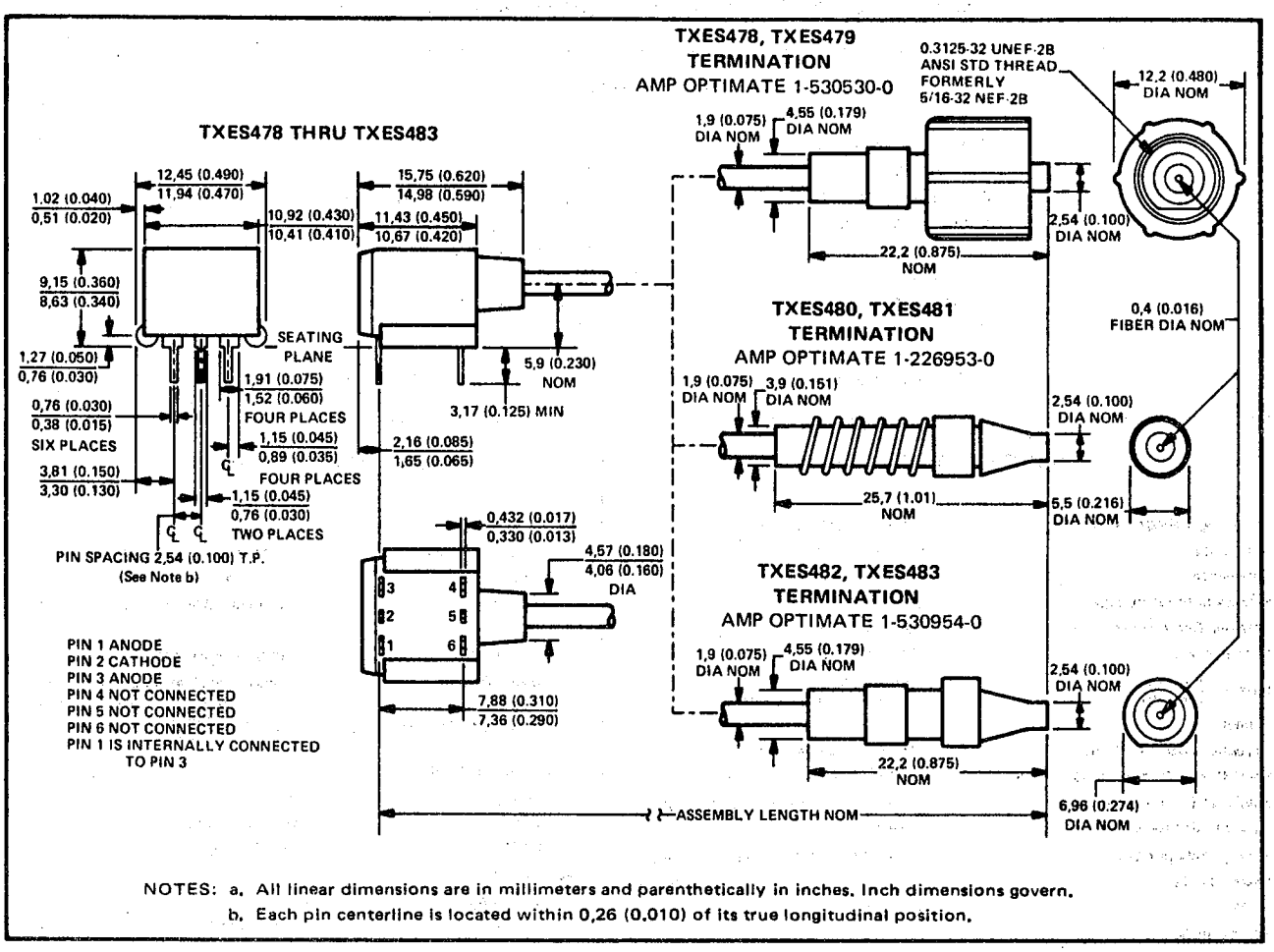

NOTES: a. All linear dimensions are in millimeters and parenthetically in inches. Inch dimensions govern.
b. Each pin centerline is located within 0,26 (0.010) of its true longitudinal position.

absolute maximum ratings

Reverse Voltage at 25°C Free-Air Temperature	2 V
Continuous Forward Current at (or below) 25°C Free-Air Temperature (See Note 1)	100 mA
Operating Free-Air Temperature Range	−20°C to 70°C
Storage Temperature Range	−20°C to 70°C
Lead Temperature 1/16 Inch (1,6 mm) below Seating Plane for 3 Seconds	230°C

NOTE 1: Derate linearly to 55 mA at 70°C free-air temperature at the rate of 1 mA/°C.

Table 5 **SERIES TXES478 THRU TXES483**

operating characteristics at 25°C free-air temperature

PARAMETER		TEST CONDITIONS	TXES478C025			TXES478C050			TXES478C100			TXES479C025			TXES479C050			TXES479C100			UNIT
			MIN	TYP	MAX	MIN	TYP	MAX	MIN	TYP	MAX	MIN	TYP	MAX	MIN	TYP	MAX	MIN	TYP	MAX	
P_O	Source Assembly Radiant Power Output	I_F = 100 mA*	80	120		75	110		65	100		160	200		145	180		130	165		μW
I_e	Axial Radiant Intensity			150			146			136			250			242			228		μW/sr
λ_p	Wavelength at Peak Emission		770	790	810	770	790	810	770	790	810	770	790	810	770	790	810	770	790	810	nm
$\Delta\lambda$	Spectral Bandwidth			40			40			40			40			40			40		nm
θ_{HI}	Half-Intensity Beam Angle			56°			52°			50°			56°			52°			50°		
V_F	Static Forward Voltage			1.6	2		1.6	2		1.6	2		1.6	2		1.6	2		1.6	2	V
C	Capacitance	V_F = 0		200			200			200			200			200			200		pF
t_r	Radiant Pulse Rise Time§	I_F = 100 mA, See Figure 1		20	30		20	30		20	30		20	30		20	30		20	30	ns

operating characteristics at 25°C free-air temperature

PARAMETER		TEST CONDITIONS	TXES480C005 TXES482C005			TXES480C010 TXES482C010			TXES480C025 TXES482C025			TXES481C005 TXES483C005			TXES481C010 TXES483C010			TXES481C025 TXES483C025			UNIT
			MIN	TYP	MAX	MIN	TYP	MAX	MIN	TYP	MAX	MIN	TYP	MAX	MIN	TYP	MAX	MIN	TYP	MAX	
P_O	Source Assembly Radiant Power Output	I_F = 100 mA*	90	135		85	130		80	120		180	225		170	215		160	200		μW
I_e	Axial Radiant Intensity			154			152			150			256			254			250		μW/sr
λ_p	Wavelength at Peak Emission		770	790	810	770	790	810	770	790	810	770	790	810	770	790	810	770	790	810	nm
$\Delta\lambda$	Spectral Bandwidth			40			40			40			40			40			40		nm
θ_{HI}	Half-Intensity Beam Angle			60°			59°			56°			60°			59°			56°		
V_F	Static Forward Voltage			1.6	2		1.6	2		1.6	2		1.6	2		1.6	2		1.6	2	V
C	Capacitance	V_F = 0		200			200			200			200			200			200		pF
t_r	Radiant Pulse Rise Time§	I_F = 100 mA, See Figure 1		20	30		20	30		20	30		20	30		20	30		20	30	ns

*Recommended operating conditions are I_F = 100 mA with a maximum duty cycle of 50%.

§The radiant pulse fall time is approximately equal to the rise time. The typical electrical bandwidth (in MHz) at which the radiant power output is reduced to $1/\sqrt{2}$ of the maximum low-frequency value is approximately $350/t_r$ (t_r in ns), or 18 MHz. The typical optical bandwidth at which the radiant power output is reduced to 1/2 of the maximum low-frequency value is approximately $610/t_r$, or 30 MHz.

FIBER-OPTIC SILICON DETECTOR ASSEMBLIES

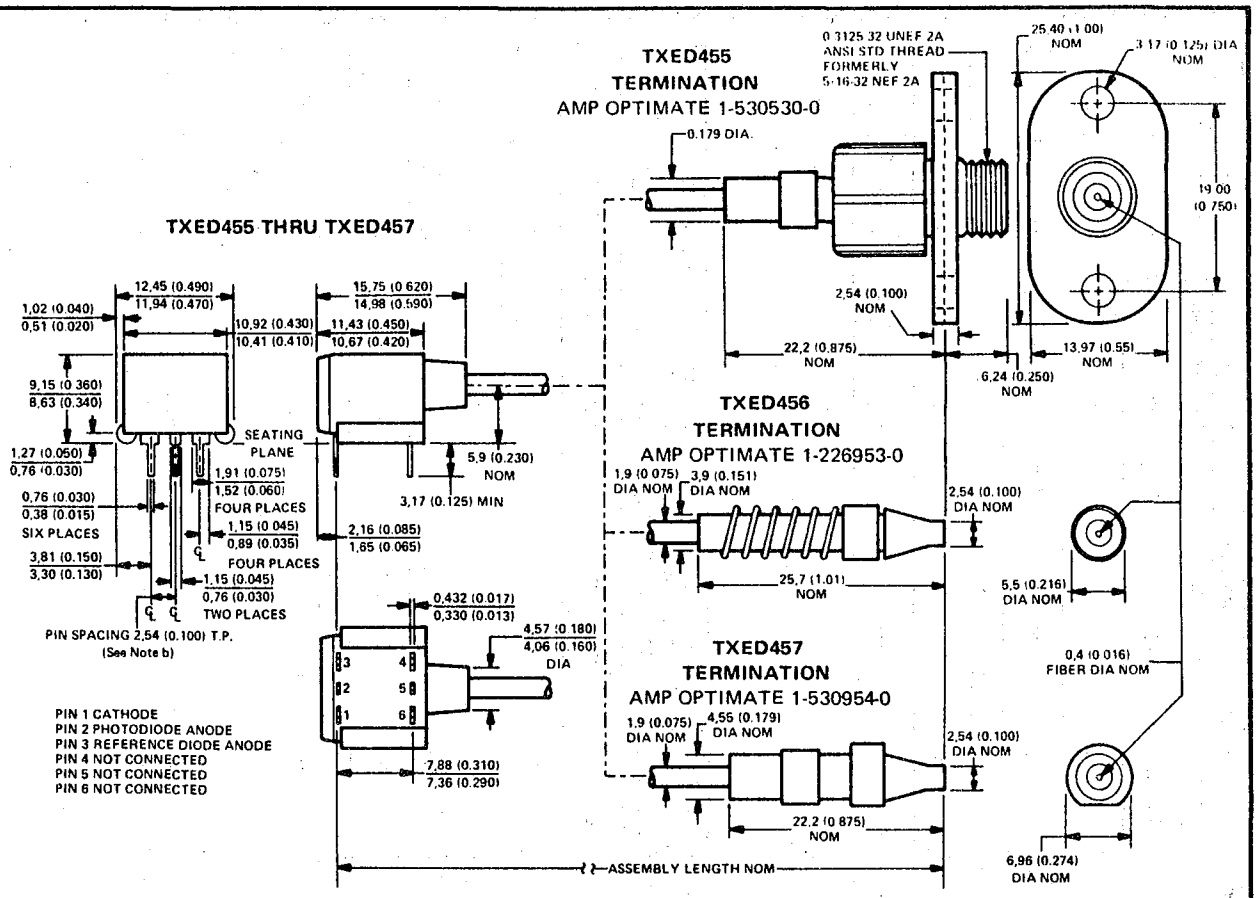

NOTES: a. All linear dimensions are in millimeters and parenthetically in inches. Inch dimensions govern.
b. Each pin centerline is located within 0,26 (0.010) of its true longitudinal position.

absolute maximum ratings

Continuous Power Dissipation at (or below) 25°C Free-Air Temperature (See Note 1)	100 mW
Operating Free-Air Temperature Range	−20°C to 70°C
Storage Temperature Range	−20°C to 70°C
Lead Temperature 1/16 Inch (1,6 mm) Below Seating Plane for 3 Seconds	230°C

NOTE 1: Derate linearly to 55 mW at 70°C at the rate of 1 mW/°C.

operating characteristics at 25°C free-air temperature

PARAMETER		TEST CONDITIONS		TXED455C025			TXED455C050			TXED455C100			TXED456C005 TXED457C005			TXED456C010 TXED457C010			TXED456C025 TXED457C025			UNIT
				MIN	TYP	MAX	MIN	TYP	MAX	MIN	TYP	MAX	MIN	TYP	MAX	MIN	TYP	MAX	MIN	TYP	MAX	
$V_{(BR)}$	Breakdown Voltage†	I_R = 100 μA, E_e = 0, See Note 2		50	100		50	100		50	100		50	100		50	100		50	100		V
I_D	Dark Current†	V_R = 25 V, E_e = 0			4	15		4	15		4	15		4	15		4	15		4	15	nA
	Dark Current Differential‡	V_R = 25 V, E_e = 0			0	±2		0	±2		0	±2		0	±2		0	±2		0	±2	nA
C_T	Total Capacitance†	V_R = 5 V, E_e = 0			2.3			2.3			2.3			2.3			2.3			2.3		pF
$R_{e(d)}$	Detector Radiant Responsivity	V_R = 5 V, λ = 850 nm			0.57			0.57			0.57			0.57			0.57			0.57		A/W
$R_{e(a)}$	Detector Assembly Radiant Responsivity	V_R = 5 V, See Note 3		0.24	0.30		0.22	0.28		0.2	0.25		0.23	0.31		0.23	0.31		0.22	0.30		A/W
t_r	Rise Time¶	See Figure 1	V_R = 5 V		8	12		8	12		8	12		8	12		8	12		8	12	ns
			V_R = 12 V		5			5			5			5			5			5		
			V_R = 25 V		3			3			3			3			3			3		

†These parameters are measured for the photodiode and the reference diode, separately.

‡Dark current differential is the difference between the dark currents of the photodiode and the reference diode.

¶The fall time is approximately equal to the rise time. The typical electrical bandwidth (in MHz) at which the detector current output is reduced to $1/\sqrt{2}$ of the maximum low-frequency value is approximately $350/t_r$ (t_r in ns). The typical optical bandwidth at which the detector current output is reduced to 1/2 of the maximum low-frequency value is approximately $610/t_r$.

NOTES: 2. Irradiance (E_e) is the radiant power per unit area incident on the surface.

3. The detector assembly radiant responsivity measurement is made with the optical input of the detector assembly attached to the optical output of a compatible fiber-optic GaAlAs source assembly with an integral fiber-optic assembly length of 25 centimeters and with a peak emission wavelength of 850 nanometers. The detector assembly radiant responsivity $R_{e(a)}$ is defined as the detector current output divided by P_O, which is the source assembly radiant power output. This parameter includes the connector coupling loss and the fiber attenuation loss.

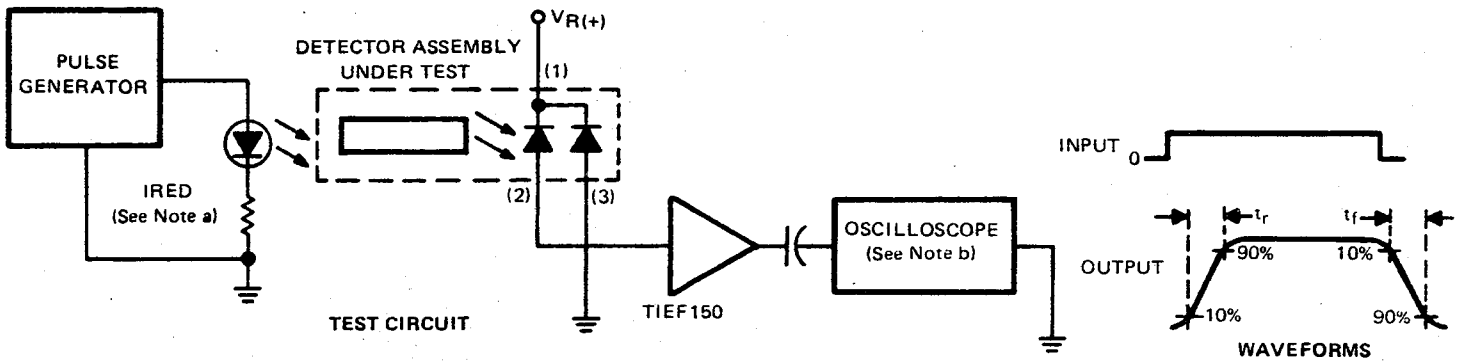

NOTES: a. Input irradiance is supplied by a pulsed GaAlAs infrared emitting diode with the following operating characteristics: λ_p = 850 nm, $t_w \leq 200$ ns, $t_r \leq 4$ ns.

b. The output waveform is monitored on an oscilloscope with the following characteristics: Z_{in} = 50 Ω, $t_r \leq 2$ ns. The measured rise time is corrected for the combined rise times of the optical source, the TIEF150 transimpedance amplifier, and the oscilloscope.

FIGURE 1–SWITCHING TIMES

Table 8

PIFAX* S-120 type 30

fiber optic cable

PIFAX* S-120 type 30 fiber optic cable is a single channel, multimode, step-index, silica-core cable. The optical fiber is clad with a tough hard plastic which can be attached directly to connectors. The silica core has minimum attenuation increase when exposed to nuclear radiation.

NOMINAL PHYSICAL DIMENSIONS

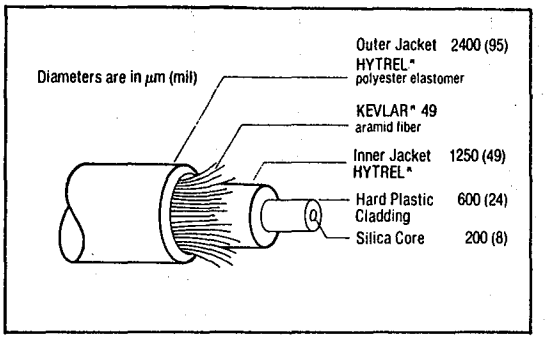

MAXIMUM SPECTRAL ATTENUATION†

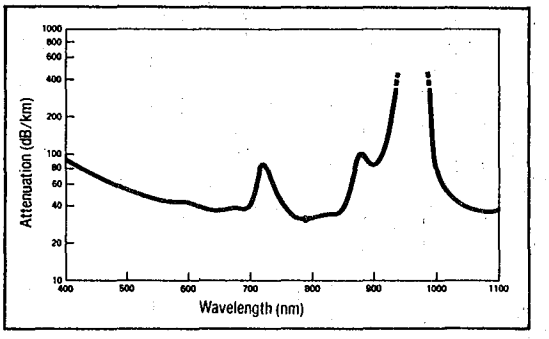

PRODUCT CHARACTERISTICS

DESCRIPTION	TYPICAL	MAXIMUM	UNITS	TEST CONDITIONS	NOTES
Attenuation	35		dB/km	670 nm	1
Attenuation	25	30	dB/km	790 nm	1
Attenuation	30		dB/km	820 nm	1,4
Attenuation	95		dB/km	900 nm	1
Numerical Aperture	0.42			material	
Numerical Aperture	0.38			10% intensity	1
Core Refractive Index	1.46				
Risetime (10-90%)	7-8		ns/0.2 km	RCA C30133	
Core Concentricity	11	18	%	based on core diameter	
Core Diameter	200		μm		
Fiber Diameter	600		μm		
Outer Jacket Diameter	2400		μm		
Bend Radius	1.5		mm	short term	2
Bend Radius	3.2		mm	long term	5
Cable Break Strength	65		kg		
Cable Flex Resistance	10000		cycles		3
Cable Weight	6		kg/km		

Notes:

1. Steady state values using monochromator (± 2 nm).
2. Cable can be wrapped 3 times around a 1.5 mm radius mandrel with no fiber breakage.
3. DOD-STD-1678 method 2010.
4. Cable typical attenuation at 820 nm after 12 days exposure 70°C/90% RH is unchanged. Optical fiber meets typical attenuation specifications after 20 months immersion in water at room temperature.
5. Cable wrapped around 3.2 mm radius mandrels with no fiber breakage after eight months.

*Du Pont's Trademark

†Curve shown is typical steady-state attenuation of sample at maximum shipping limit of 30 dB·km at 790nm using a monochromator

DUPONT

Table 9

SPECIFICATIONS

DC* POWER RANGES: -90dBm to +3dBm
-60dBu to +33dBμ

AC POWER RANGES: -80dBm to -10dBm
-50dBu to +20dBμ

FREQUENCY RESPONSE: DC to unlimited AC

ACCURACY: ± 1% of reference level (+3 to -80dBm)
±10% of reference level (-80 to -90dBm)

CONSTANT CURRENT OUTPUT: 25ma nominal

DIGITAL OUTPUTS: Multiplexed 7 Segment, digital ground.

ANALOG OUTPUTS: Log of SIG.IN, Log of REF.IN, ground, V+, V-

SAMPLE/HOLD DRIFT: .1dB/3 minutes

BATTERY: 7.2 volt, Eveready CH22, Ni-Cd rechargeable

BATTERY LIFE: 9 hours nominal -
3 hours with current source on

DIMENSIONS: Length 7.35 in. (18.7mm)
Width 4.45 in. (11.3mm)
Height 1.70 in. (4.3mm)

WEIGHT: 0.6 Kg. (1 lb. 4 oz.)

SHIPPING WIEGHT: 1.8 Kg (4 lbs.)

OPERATING TEMPERATURE: 0 to 55°C

NOTE: The Model 22XL does not separate DC and AC signals. AC average power measurements between 100 Hz and 1 MHz are correctly indicated only with the AC button in, although a reading will appear on DC. AC frequencies above 1 MHz will be correctly indicated on either AC or DC.

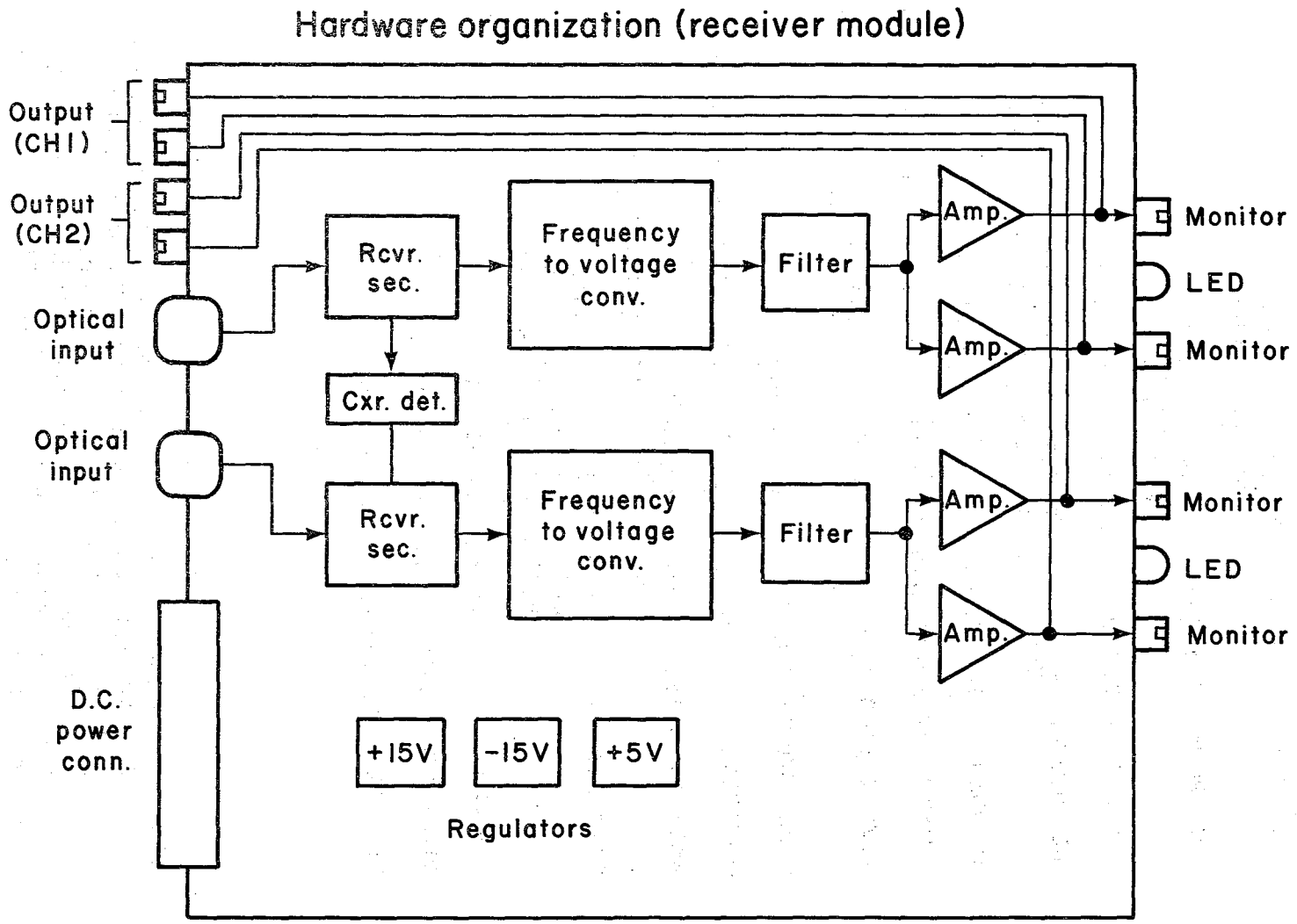

Figure 1

XBL 8112-13231

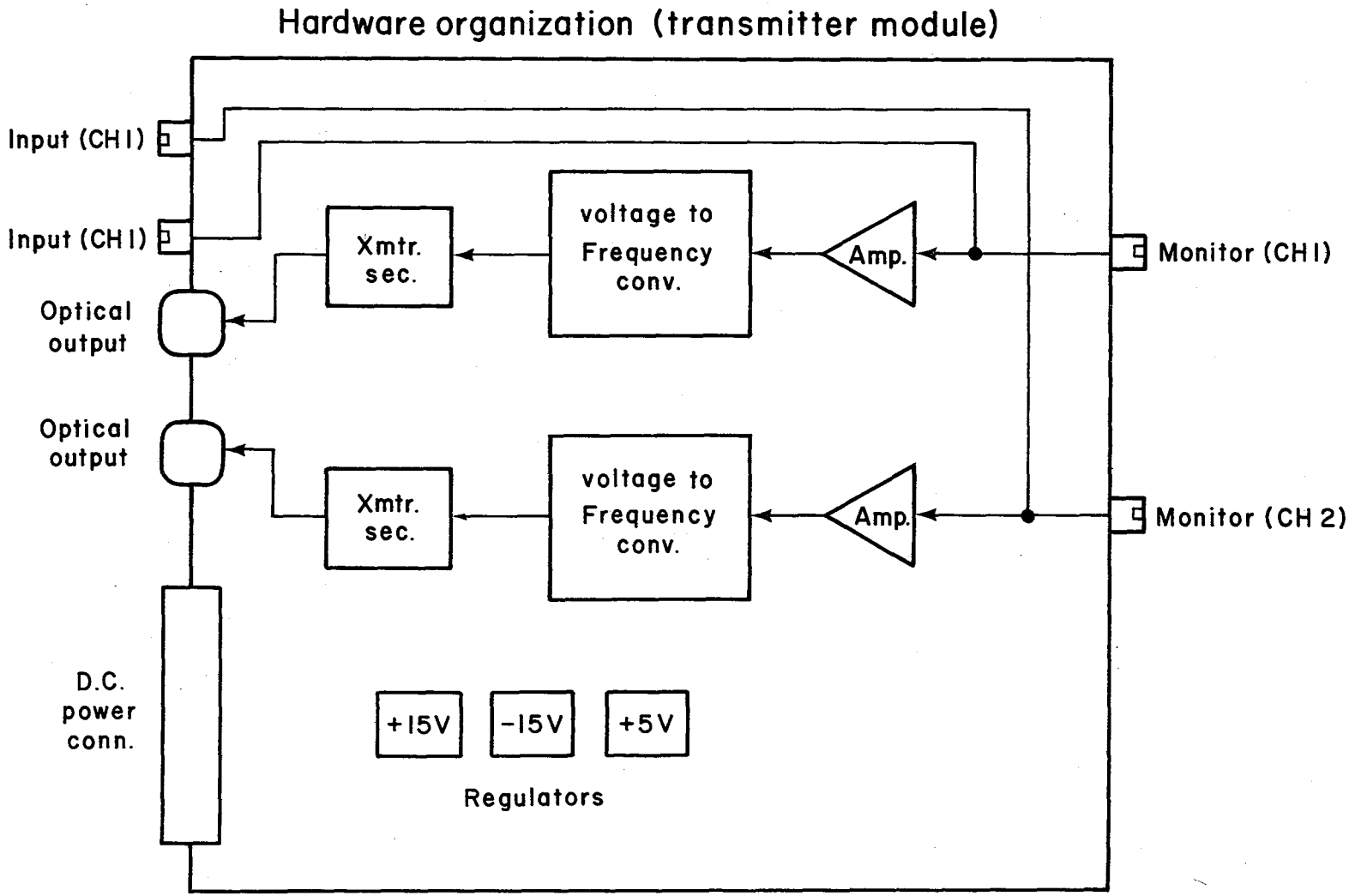

Figure 2

XBL 8112-13232

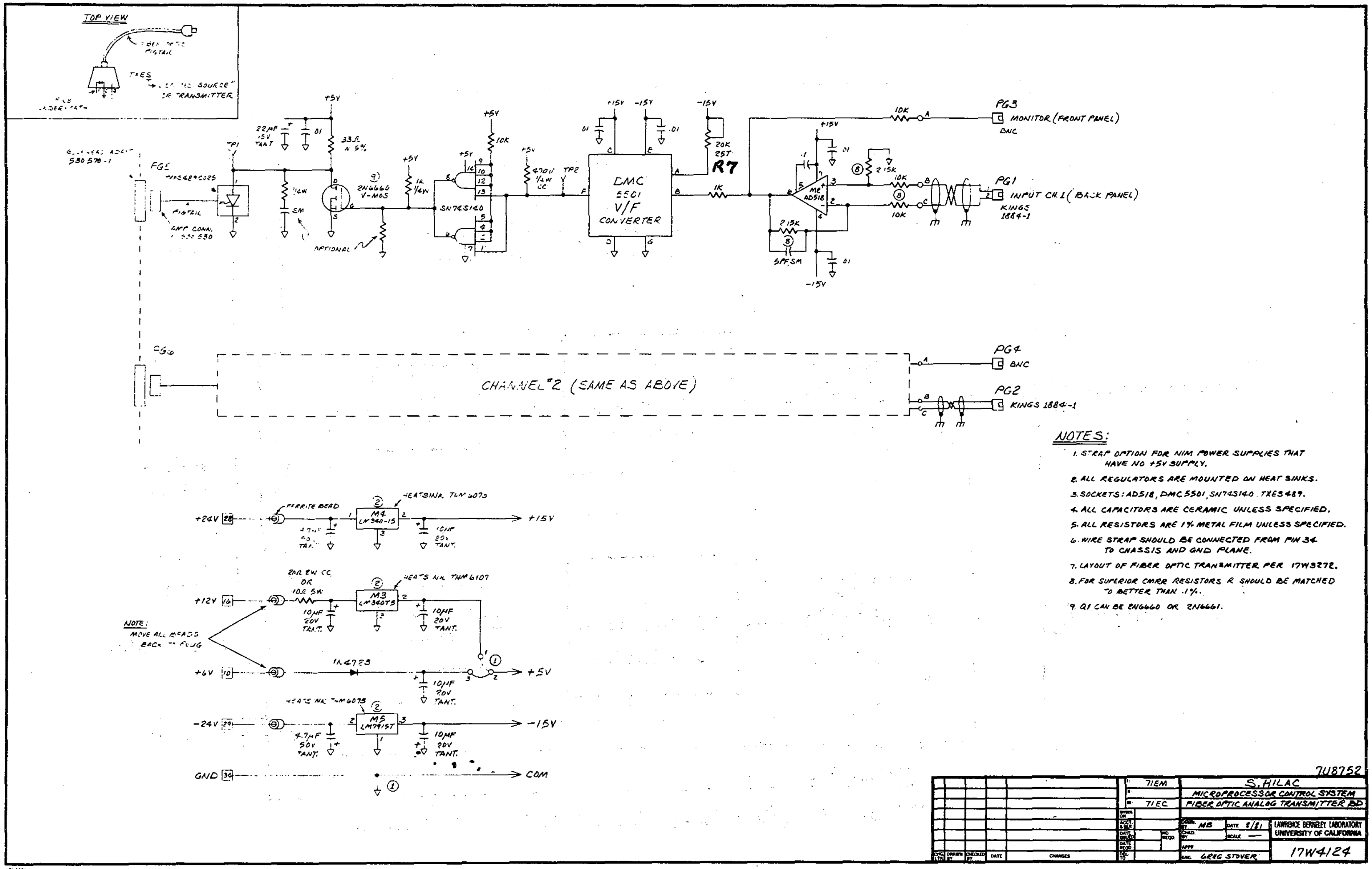
TOP VIEW
FG5
PG3
MONITOR (FRONT PANEL)
BNC
PG1
INPUT CH.1 (BACK PANEL)
KINGS
1884-1
PG4
BNC
PG2
KINGS 1884-1
DMC
5501
V/F
CONVERTER
R7
SN74S140
2N6660
V-MOS
OPTIONAL
CHANNEL #2 (SAME AS ABOVE)
FERRITE BEAD
M4
LM340-15
M3
LM340T5
M5
LM7915T
1N4723
+24V
+12V
+6V
-24V
GND
+15V
+5V
-15V
COM
NOTE:
MOVE ALL BEADS BACK TO PLUG
NOTES:
1. STRAP OPTION FOR NIM POWER SUPPLIES THAT HAVE NO +5V SUPPLY.
2. ALL REGULATORS ARE MOUNTED ON HEAT SINKS.
3. SOCKETS: AD518, DMC5501, SN74S140. TXE5489.
4. ALL CAPACITORS ARE CERAMIC UNLESS SPECIFIED.
5. ALL RESISTORS ARE 1% METAL FILM UNLESS SPECIFIED.
6. WIRE STRAP SHOULD BE CONNECTED FROM PIN 34 TO CHASSIS AND GND PLANE.
7. LAYOUT OF FIBER OPTIC TRANSMITTER PER 17W3272.
8. FOR SUPERIOR CMRR RESISTORS R SHOULD BE MATCHED TO BETTER THAN .1%.
9. Q1 CAN BE 2N6660 OR 2N6661.
7U8752
S. HILAC
MICROPROCESSOR CONTROL SYSTEM
FIBER OPTIC ANALOG TRANSMITTER BD
LAWRENCE BERKELEY LABORATORY
UNIVERSITY OF CALIFORNIA
GREG STOVER
17W4124

Schematic #1

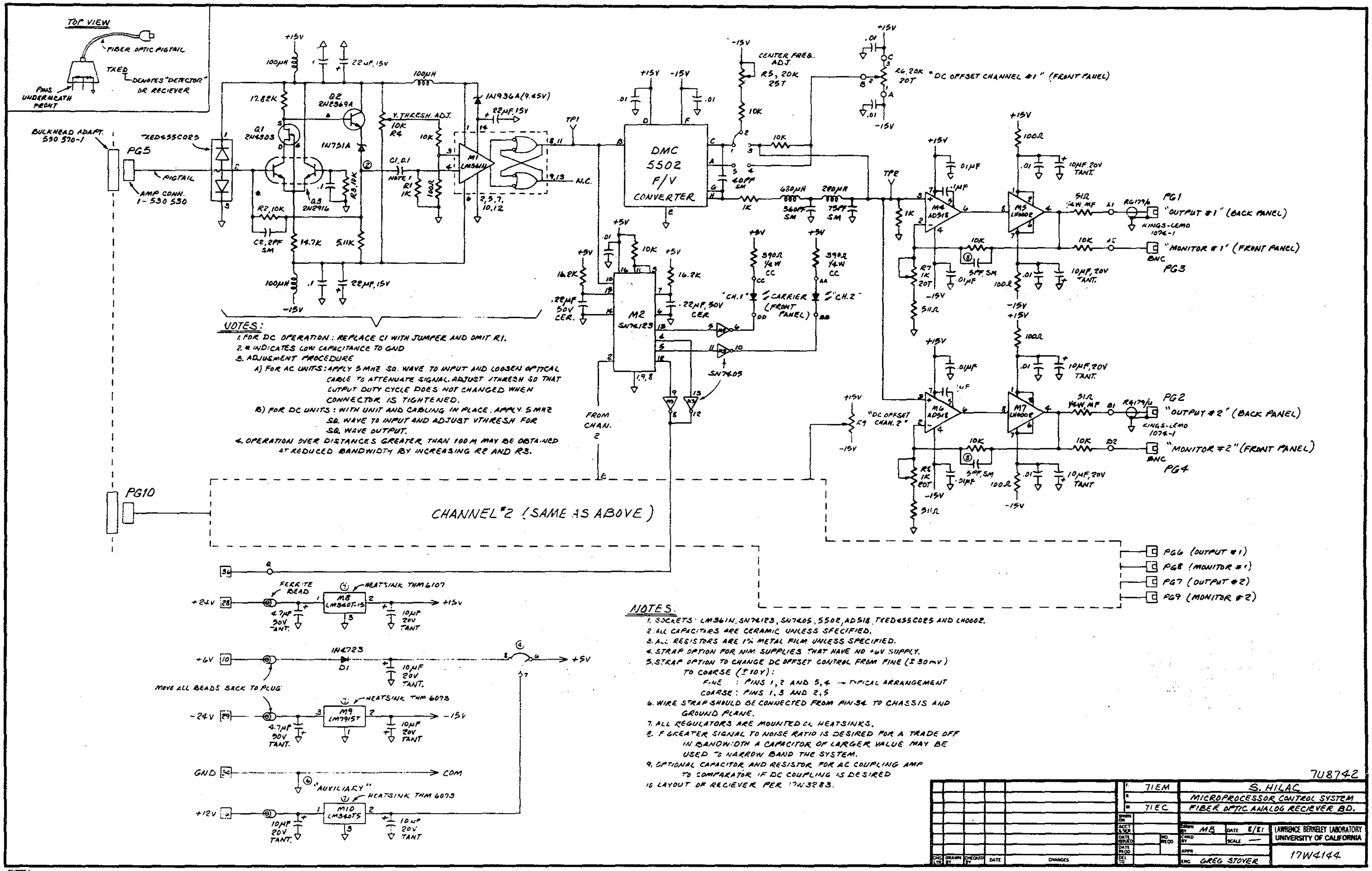
TOP VIEW
FIBER OPTIC PIGTAIL
TXED DENOTES "DETECTOR" OR RECIEVER
PINS UNDERNEATH FRONT
BULKHEAD ADAPT. 530 570-1
PG5
TXED455C025
PIGTAIL
AMP CONN. 1-530 530
DMC 5502 F/V CONVERTER
CENTER FREQ. ADJ.
R5, 20K 25T
R6, 20K 20T
"DC OFFSET CHANNEL #1" (FRONT PANEL)
V. THRESH. ADJ.
1N934A(9.45V)
1N731A
Q1 2N4303
Q2 2N5369A
Q3 2N2916
M1 LM361N
M2 SN74123
SN7405
"CH.1" CARRIER (FRONT PANEL) "CH.2"
M4 AD518
M5 LH0002
M6 AD518
M7 LH0002
PG1 "OUTPUT #1" (BACK PANEL)
KINGS-LEMO 1074-1
"MONITOR #1" (FRONT PANEL)
BNC
PG3
PG2 "OUTPUT #2" (BACK PANEL)
"MONITOR #2" (FRONT PANEL)
PG4
"DC OFFSET CHAN. 2"
FROM CHAN. 2
NOTES:
1. FOR DC OPERATION: REPLACE C1 WITH JUMPER AND OMIT R1.
2. * INDICATES LOW CAPACITANCE TO GND
3. ADJUSMENT PROCEDURE
A) FOR AC UNITS: APPLY 5 MHZ SQ. WAVE TO INPUT AND LOOSEN OPTICAL CABLE TO ATTENUATE SIGNAL. ADJUST VTHRESH SO THAT OUTPUT DUTY CYCLE DOES NOT CHANGED WHEN CONNECTOR IS TIGHTENED.
B) FOR DC UNITS: WITH UNIT AND CABLING IN PLACE, APPLY 5 MHZ SQ. WAVE TO INPUT AND ADJUST VTHRESH FOR SQ. WAVE OUTPUT.
4. OPERATION OVER DISTANCES GREATER THAN 100 M MAY BE OBTAINED AT REDUCED BANDWIDTH BY INCREASING R2 AND R3.
PG10
CHANNEL #2 (SAME AS ABOVE)
PG6 (OUTPUT #1)
PG8 (MONITOR #1)
PG7 (OUTPUT #2)
PG9 (MONITOR #2)
+24V
FERRITE BEAD
HEATSINK THM 6107
M8 LM340T-15
+15V
+6V
1N4723
D1
+5V
MOVE ALL BEADS BACK TO PLUG
-24V
HEATSINK THM 6073
M9 LM7915T
-15V
GND
COM
"AUXILIARY"
+12V
M10 LM340T5
NOTES:
1. SOCKETS: LM361N, SN74123, SN7405, 5502, AD518, TXED455C025 AND LH0002.
2. ALL CAPACITORS ARE CERAMIC UNLESS SPECIFIED.
3. ALL RESISTORS ARE 1% METAL FILM UNLESS SPECIFIED.
4. STRAP OPTION FOR NIM SUPPLIES THAT HAVE NO +6V SUPPLY.
5. STRAP OPTION TO CHANGE DC OFFSET CONTROL FROM FINE (± 30mV) TO COARSE (± 10V):
FINE : PINS 1,2 AND 5,4 → TYPICAL ARRANGEMENT
COARSE: PINS 1,3 AND 2,5
6. WIRE STRAP SHOULD BE CONNECTED FROM PIN 34 TO CHASSIS AND GROUND PLANE.
7. ALL REGULATORS ARE MOUNTED ON HEATSINKS.
8. IF GREATER SIGNAL TO NOISE RATIO IS DESIRED FOR A TRADE OFF IN BANDWIDTH A CAPACITOR OF LARGER VALUE MAY BE USED TO NARROW BAND THE SYSTEM.
9. OPTIONAL CAPACITOR AND RESISTOR FOR AC COUPLING AMP TO COMPARATOR IF DC COUPLING IS DESIRED
10. LAYOUT OF RECIEVER PER 17W3283.
7U8742
71EM
71EC
S. HILAC
MICROPROCESSOR CONTROL SYSTEM
FIBER OPTIC ANALOG RECIEVER BD.
DRWN BY MB
DATE 8/81
ENG GREG STOVER
LAWRENCE BERKELEY LABORATORY
UNIVERSITY OF CALIFORNIA
17W4144

Schematic #2

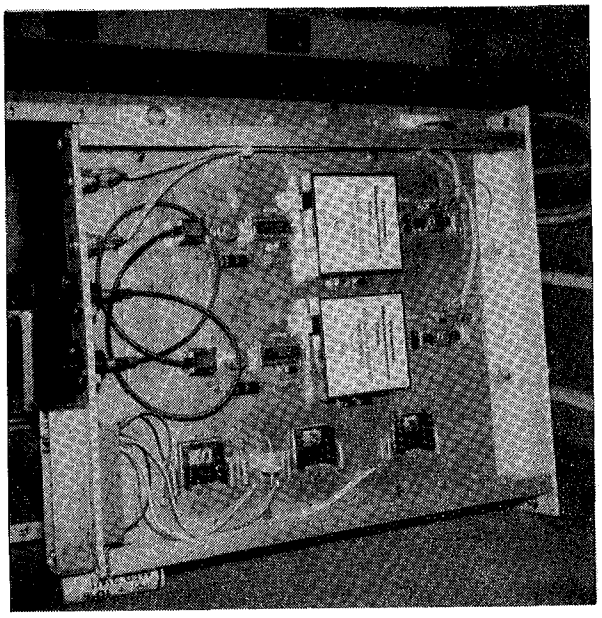

Figure 3. Transmitter module

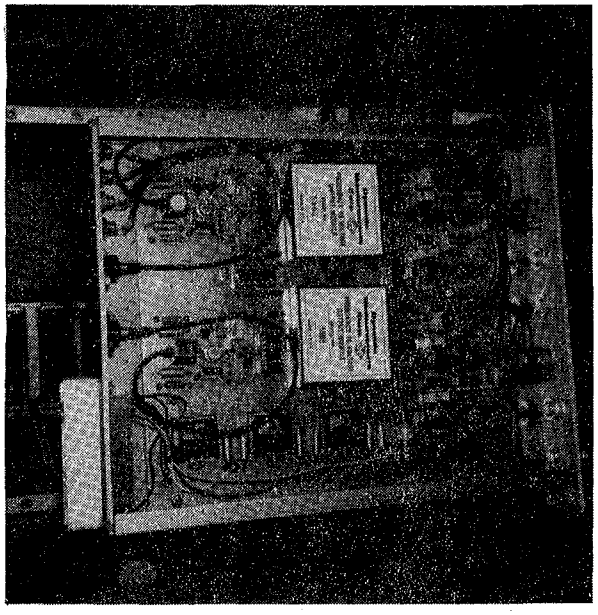

CBB 8112-11509

Figure 4. Receiver module

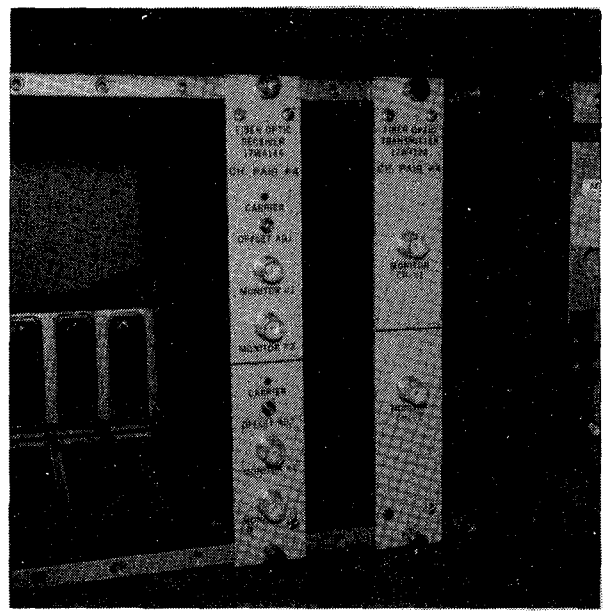

Figure 5. Transmitter, Receiver (front view)

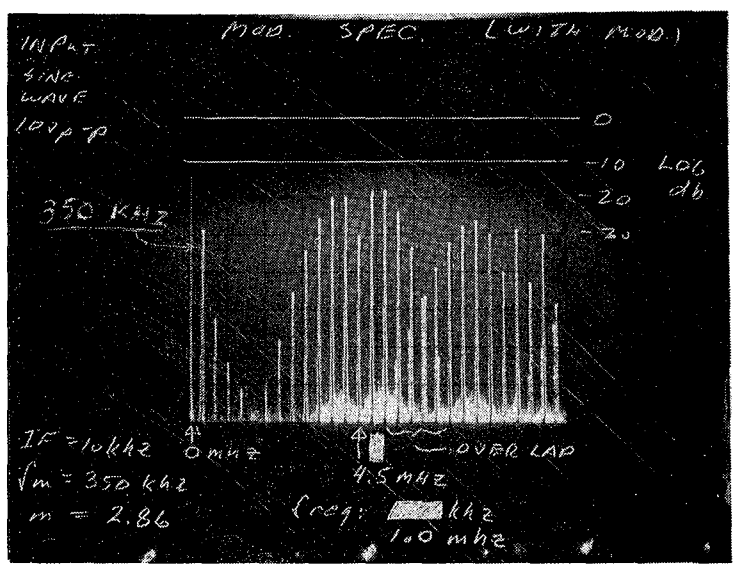

CBB 8112-11511

Figure 6. Modulation Spectrum

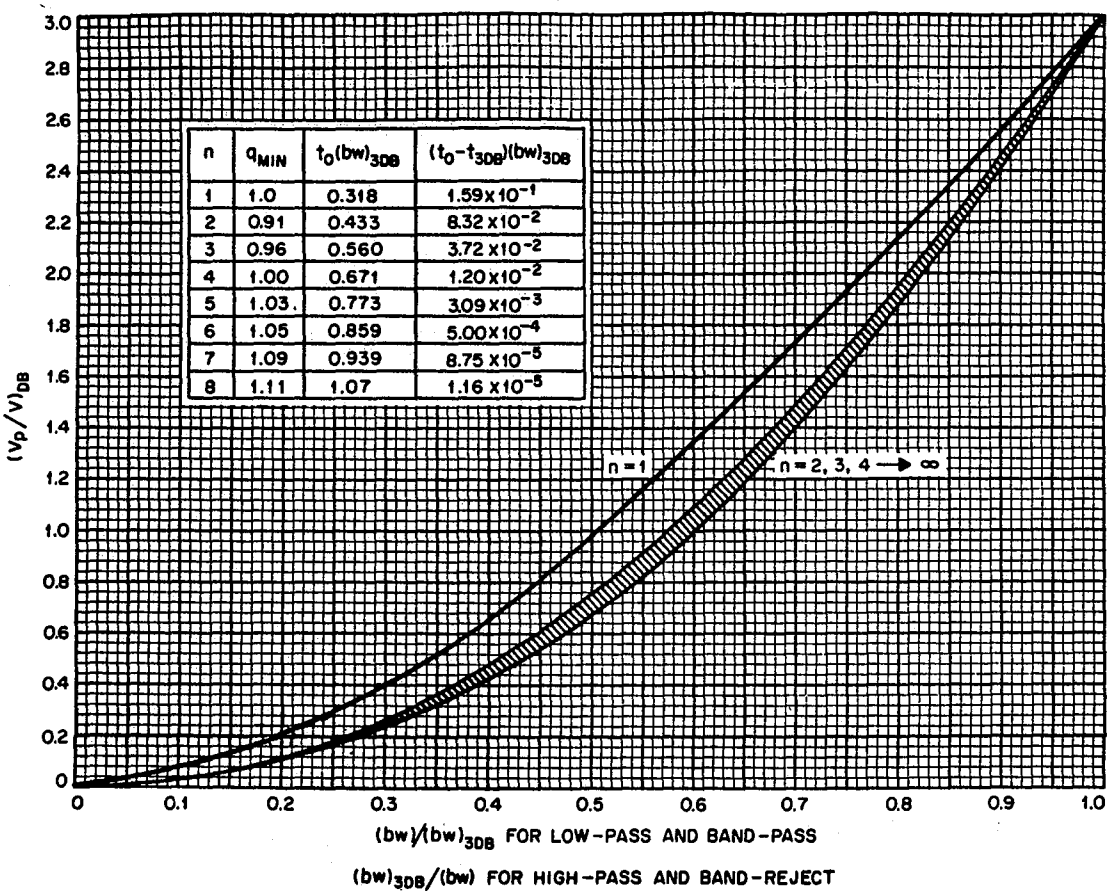

n	q_{MIN}	$t_0(bw)_{3DB}$	$(t_0-t_{3DB})(bw)_{3DB}$
1	1.0	0.318	1.59×10^{-1}
2	0.91	0.433	8.32×10^{-2}
3	0.96	0.560	3.72×10^{-2}
4	1.00	0.671	1.20×10^{-2}
5	1.03	0.773	3.09×10^{-3}
6	1.05	0.859	5.00×10^{-4}
7	1.09	0.939	8.75×10^{-5}
8	1.11	1.07	1.16×10^{-5}

—Attenuation shape within the 3-decibel-down pass band for n-pole maximally flat time-delay filters.

Figure 7. Filter response (0 - 3db)

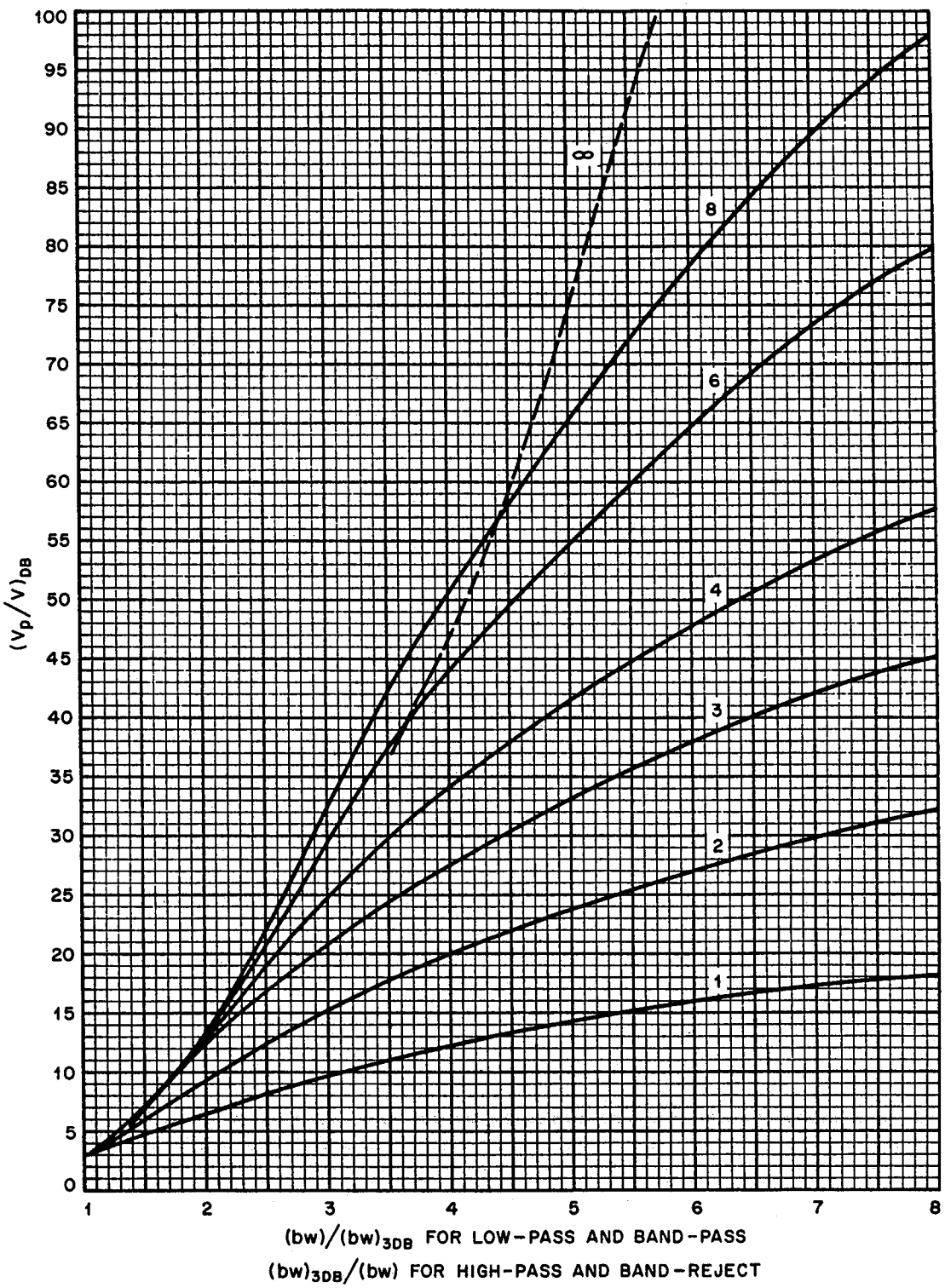

–Attenuation shape beyond 3-decibel-down pass band for n-pole maximally flat time-delay filters.

Figure 8. Filter response (3 - 100db)

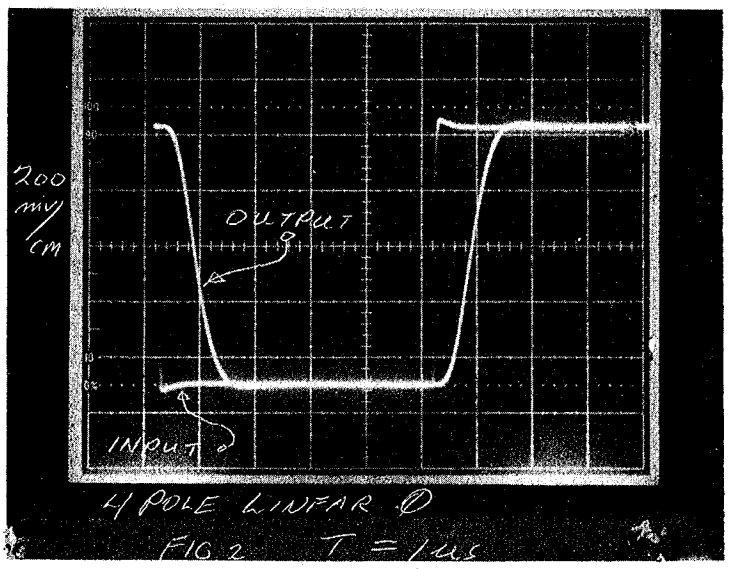

Figure 9. Filter pulse response.

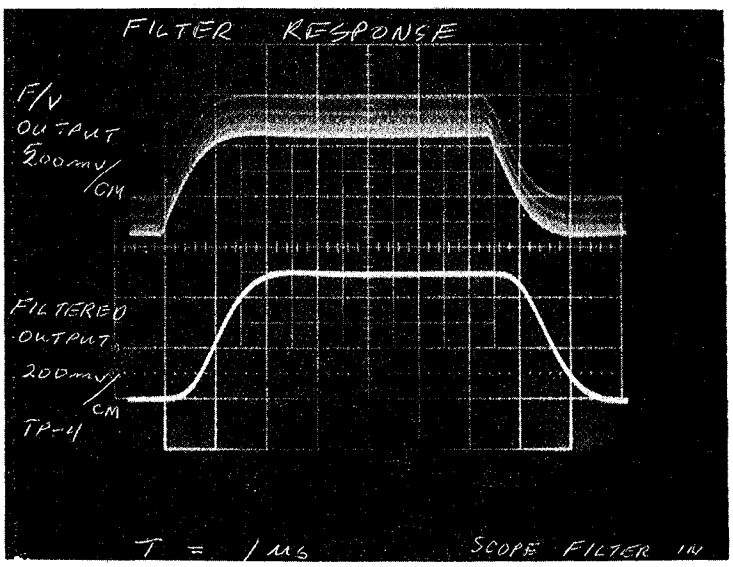

XBB 8112-11503

Figure 10. Filter response (before/after).

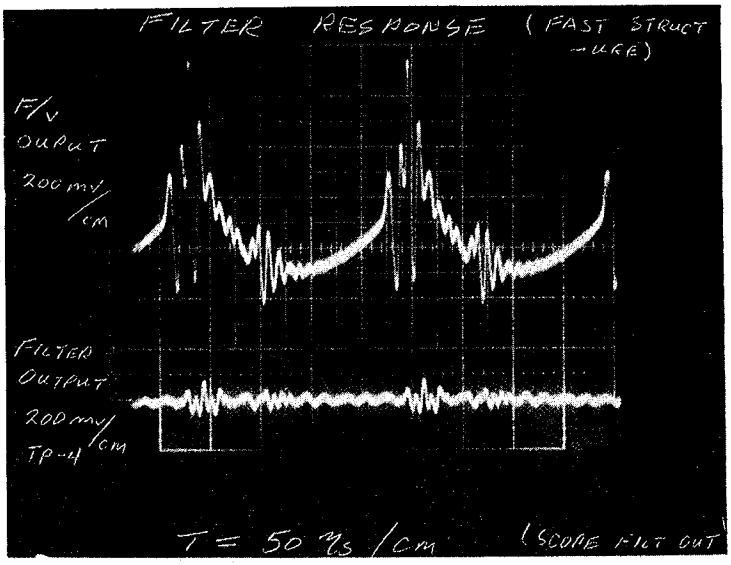

XBB 8112-11504

Figure 11. Filter response (fine structure).

Figure 12 Model 5501 Input Module

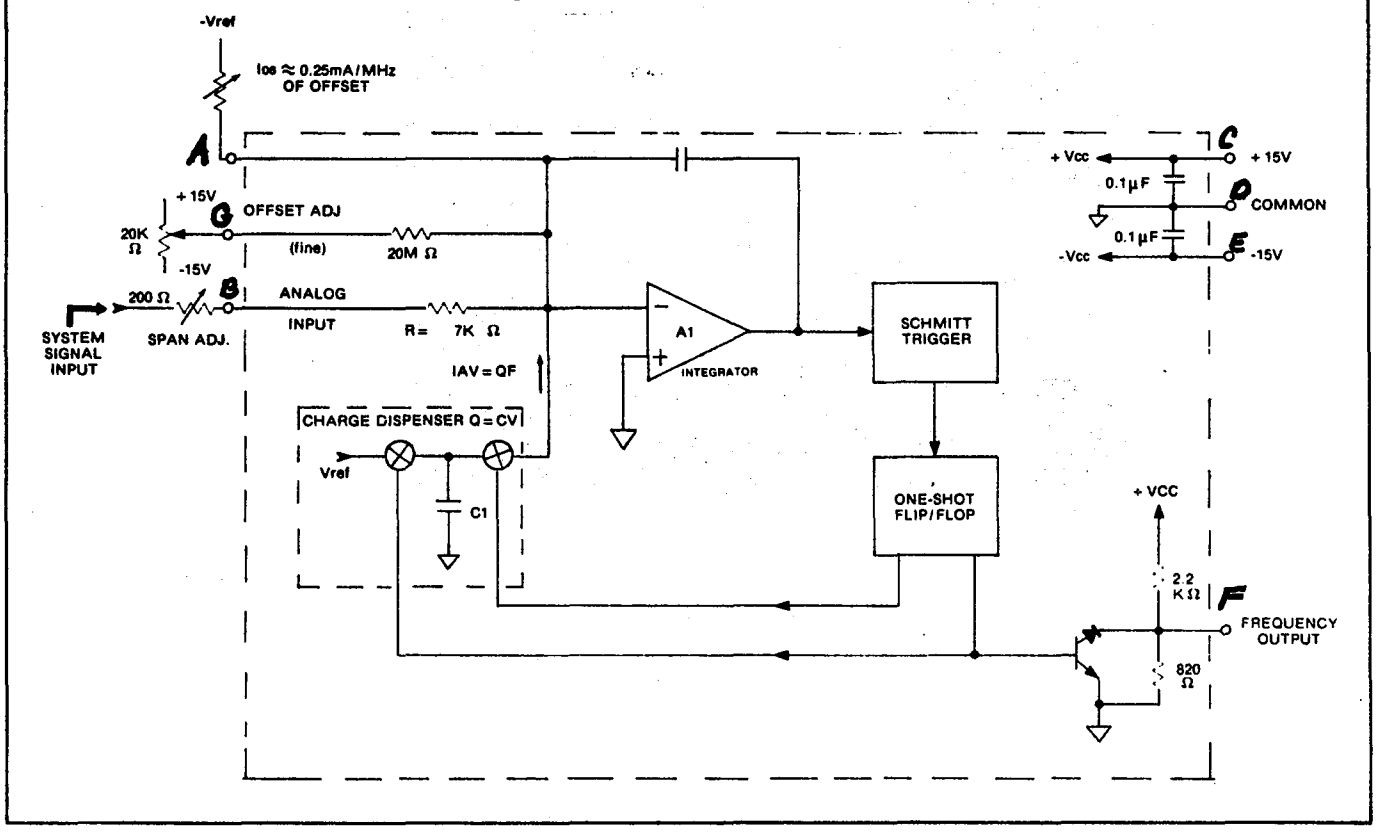

Figure 13 Model 5502 Output Module

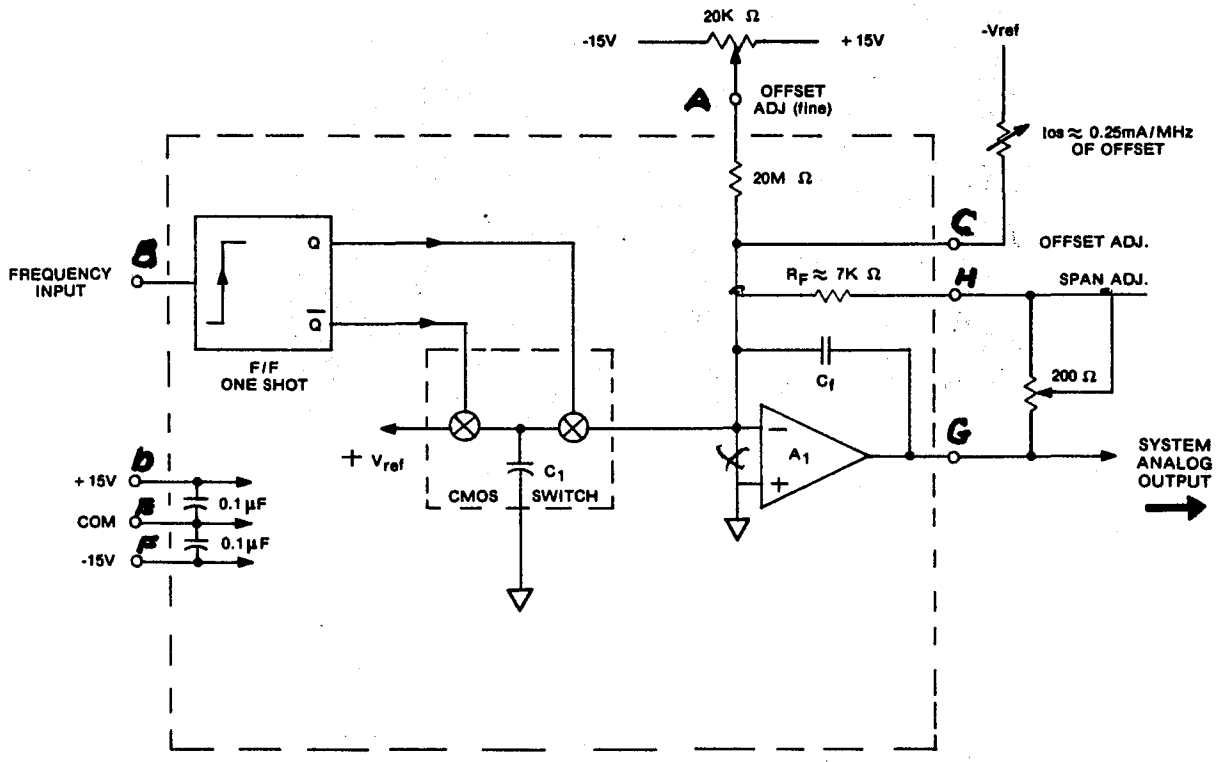

Receiver output pulse response

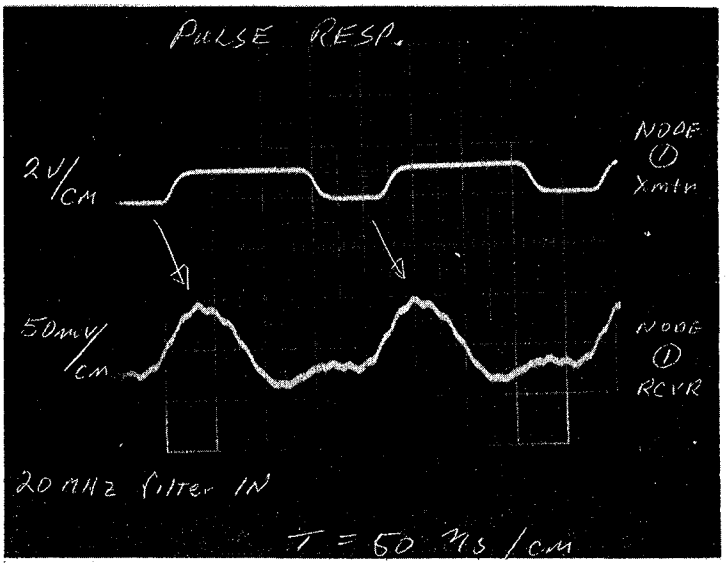

Figure 14. Receiver output, recovered carrier.

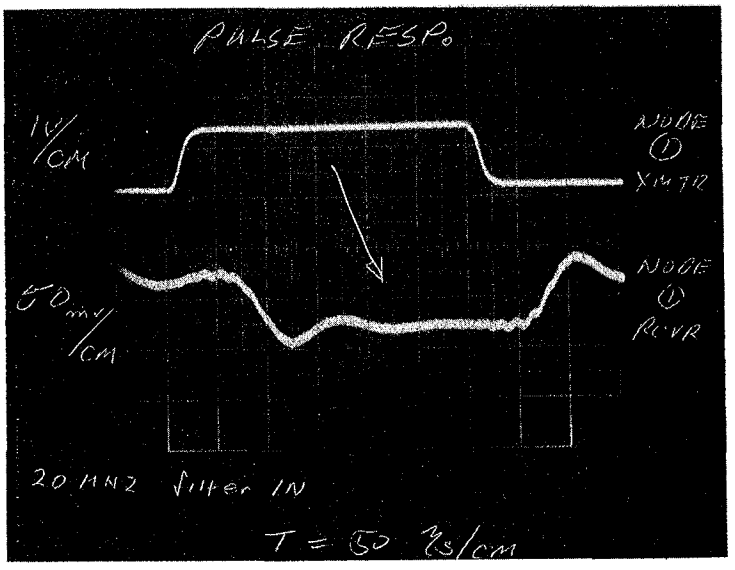

XBB 8112-11505

Figure 15. Receiver output, rise and fall times.

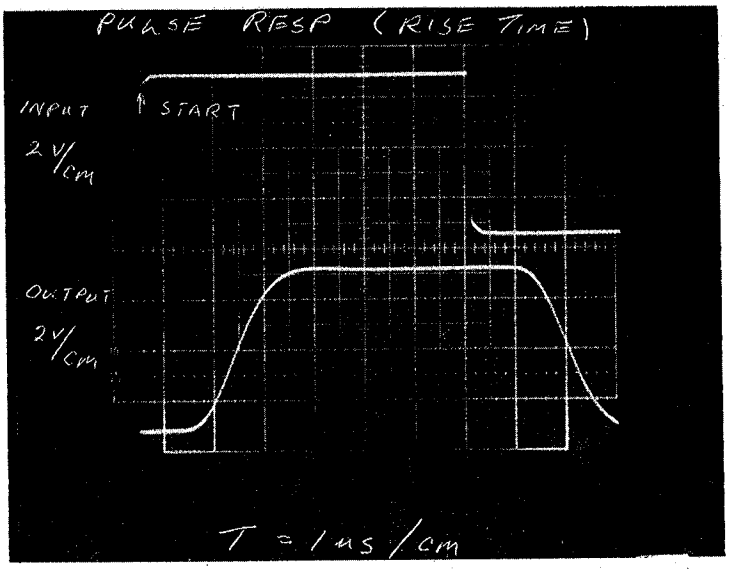

Figure 16. System large signal pulse response.

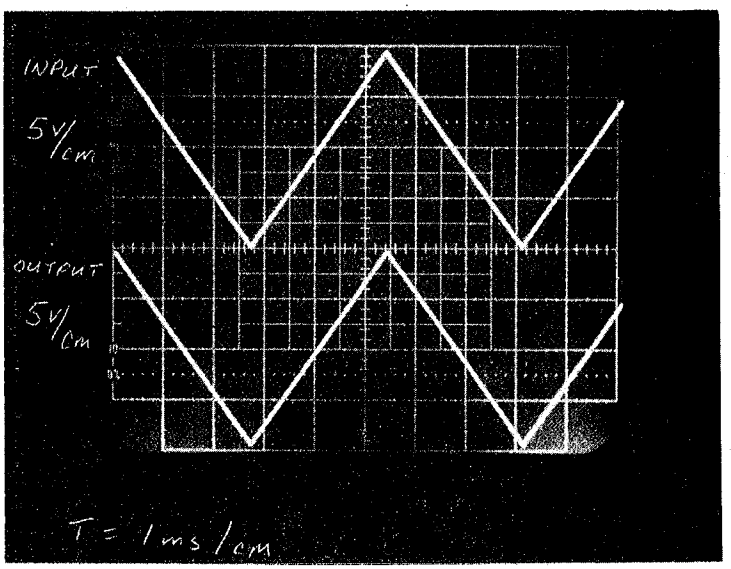

XBB 8112-11506

Figure 17. Visual linearity, input to output.

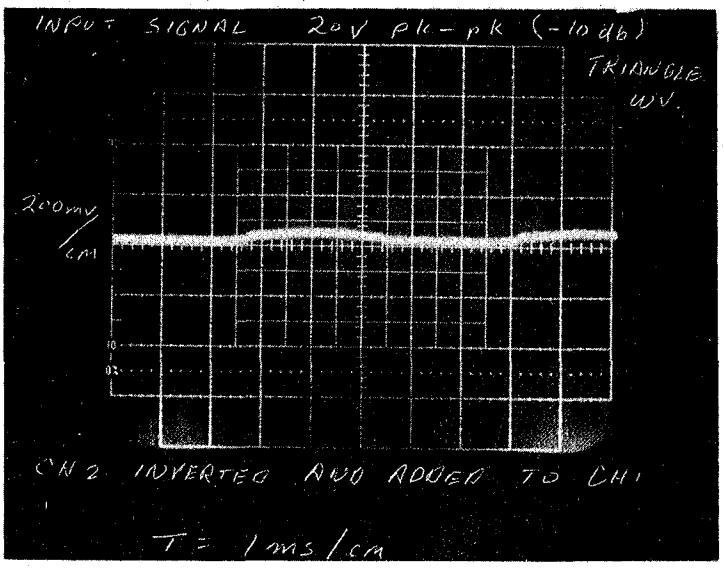

Figure 18. Gross nonlinearity

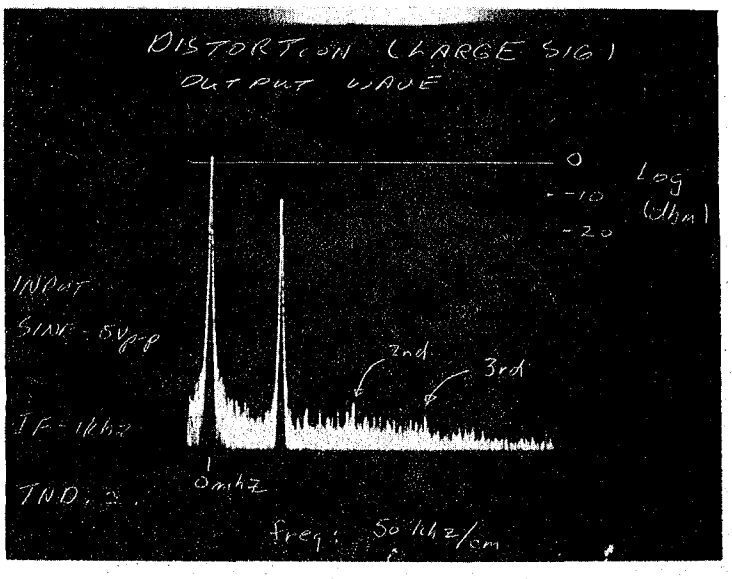

XBB 8112-11507

Figure 19. Total harmonic distortion.

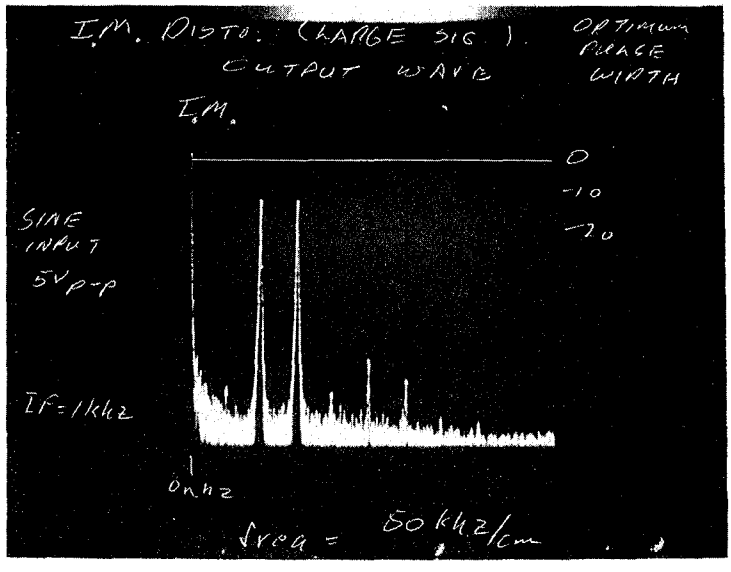

XBB 8112-11508

Figure 20. Intermodulation distortion.

APPENDIX 1

Calculation: Input noise current of fiber optic receiver preamp.

A. Differential pair surall signal parameters

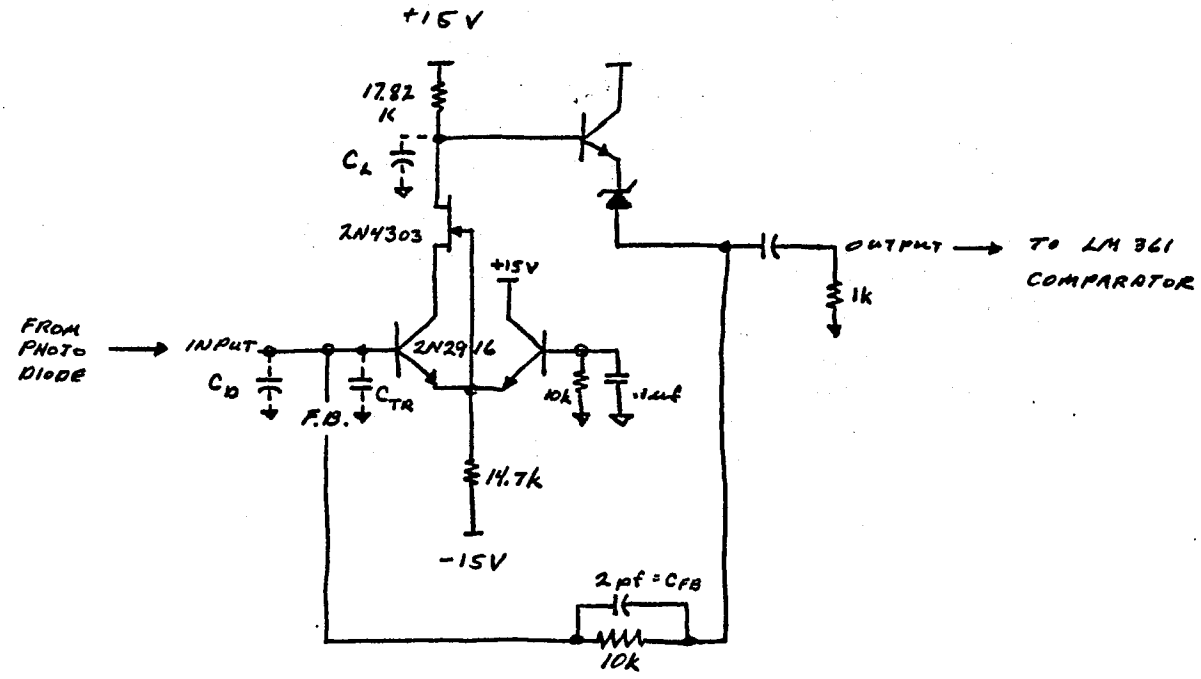

$$I_C = \frac{14.94V - 8.77V}{17.82K} = .346 \text{ ma (measured value)}$$

$$V_T \simeq .026V$$

$$Ad = \frac{.346 \text{ ma}}{.026V} 17.82 \text{ k}\Omega = 237$$

gm

$$Acm = \frac{-gm\ Rc}{1 + 2\ gm\ (RE(1 + \frac{1}{\beta_o})}$$

β_{min} | 2916 = 300

RE = 14.7 K

gm = .0133 ma/V

$$= \frac{-\ .0133\ (17.82\ k\Omega)}{1 + 2(.0133)(*14.7k\Omega)}$$

$$= .60$$

$$\frac{V_o}{V_i} = \frac{Adm}{2} + \frac{Acm}{2}$$

$$= \frac{237}{2} + \frac{.6}{2} \cong 119$$ open loop voltage gain of amplifier

B. Noise Calculation

1) Configuration of amplifier: shunt-shunt

2) Major noise components:

$$\overline{i_{int}^2} = [2q\ I_B + 4kT/R_f]\ f_w +$$

$$[4KT/gm\ (2\pi f_1 C_T)^2 + 8kT\ (r_b' + r_s)(2\pi f_1 C_b)^2]\ f_{f^2}$$

where $f_W = Nf_1$

and $f_f z = Mf_1$

and $N \simeq \tan^{-1}\left[\frac{1/a}{\pi/2 - \tan^{-1}(2a/\pi)}\right]$, $a = \frac{f_1}{f_2}$

and $M = \left[\frac{\pi}{2a_1} - \tan^{-1}\ (\frac{1}{a_1})\right]$

$C_T = C_D$ (Diode) + C_{FB} (Feedback) + C_{TR} (Trace)

$C_b = 2.2$ pf

$r_b = \frac{15V}{3.3\ na} = 4.55 \times 10^9\ \Omega$ small signal r of diode

$C_{FB} = 1$ pf NOTE: When original calculations and measurements were made C_{FB} was 1.0 pf.

$C_{TR} \simeq .3$ pf

$C_L \simeq 1.5$ pf

$$f_1 = \frac{1}{2\pi R_f C_T}$$

$$= \frac{1}{6.28\ (10k\Omega)\ 3.4\ pf}$$

$$= 4.55\ mhz$$

$$f_2 = \frac{1}{2\pi R_L C_L}$$

$$= \frac{1}{2\pi(17.82k)\ (1.5\ pf)}$$

$f_z = 5.95$ mhz $= 6.0$ mhz

$$N = \tan^{-1}\left[\frac{\frac{1}{.767}}{\pi/2 - \tan^{-1}(2/\pi\ (.767))}\right] = 1.17$$

$$a_1 = \frac{f_1}{f_2} = \frac{4.6\ mhz}{6.0\ mhz} = .767$$

$$M = \frac{\pi}{2(.767)} - \tan^{-1}\left(\frac{1}{.767}\right) = 1.13$$

$fw = 1.17\ (4.6\ mhz) = 5.4\ mhz$

$f_f 2 = 1.13\ (4.6\ mhz) = 5.2\ mhz$

$$\overline{i^2}_{shot} = 2q\ I_B fw$$

$$= 2\ (1.6 \times 10^{-19} C)\ (86.7\ \mu a)\ (5.4\ mhz)$$

$$= 1.5 \times 10^{-16}\ A^2$$

$$\overline{i^2}_{THRM.} = \frac{4kT}{R_f} fw$$

$$= \frac{4\ (1.38 \times 10^{-23})\ 300}{10k}\ (5.4 \times 10^{6})$$

$$= 8.9 \times 10^{-18}\ A^2$$

$$\overline{i^2}_{shot} = 4KT \frac{1}{gm} (2\pi f_o C_T)^2 f_f^2$$

$$= 4(300)\ 1.38 \times 10^{-23} \left(\frac{1}{.0133} \right) \cdot$$

$$(6.28\ (4.6\ mhz)\ 3.5 \times 10^{-12}\ F)^2\ 5.2\ mhz$$

$$= 6.6 \times 10^{-20}\ A^2$$

$$\overline{i^2}_{THRM} = 8\ kT\ (r_b + r_s)\ (2\pi f_2 C_D)^2\ f_f^2$$

$$= 8\ (1.38 \times 10^{-23})\ 300\ (20\Omega + 100\Omega) \cdot$$

$$(6.28\ (4.6 \times 10^{6}) 2.2 \times 10^{-12})^2\ 5.2\ mhz$$

$$= 8.35 \times 10^{-20}\ A^2$$

$$\overline{i^2}_{TOT} = 1.5 \times 10^{-16} + 6.6 \times 10^{-20} + 8.35 \times 10^{-20}$$

$$+ 8.9 \times 10^{-18}$$

$$= 1.59 \times 10^{-16}\ A^2$$

$$i_{RMS} = 1.26 \times 10^{-8} \simeq \boxed{12.6\ \eta_a}$$

B. Minimum optical input power for a signal to noise ratio = 1.

$$P_{MIN} = \frac{i_{RMS}}{Res} \qquad Res \equiv \text{responsivity}$$

$$= \frac{12.6\ \eta a}{.32\ A/W} \cdot$$

$$= 4.2 \times 10^{-8}\ w$$

$$= \boxed{42\ \eta u} \qquad \text{or} \qquad = -13.8\ db\mu w$$

Worst case optical power loss for 100 meter fiber optic cable.

A. Component specifications

1. Emitter TXED 489 - C025:

   Po (Min. at 100 ma) = 150 μw = 21.8 dbμw

   N.A. (pigtail) = .53

   Core diam. (pigtail) = Length (pigtail) = 25 cm

   Loss (pigtail) = .1db

   emitter (nom.) = 820 ηm

2. Detector TXED 455 - C025:

   R = .3 A/w at 850 ηm

   N.A. (pigtail) = .53

   Core diam. (pigtail) = 400 μm

   Loss (pigtail) = .1 db

3. Connectors AMP plastic:

   Gap (typ.) = 0.15 mm

   Misalignment (typ.) = .05 mm

4. Fiber Cable PFX S120 Type 30:

   Length = 100 m

   Attenuation at 790 η_m = 3db (1.5 db at 50m)

   N. A. = .38

   Core dia. = 200 μm

   Core concentricity = 0.36 mm

B. System Configuration:

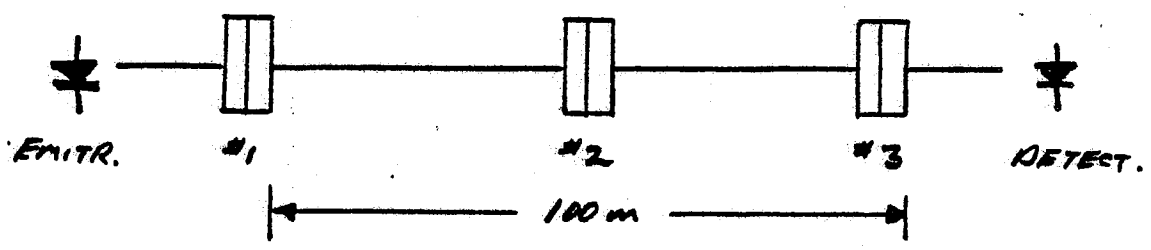

C. Loss Calculations Connectors:

		No. 1 (db)	No. 2 (db)	No. 3 (db)
a)	Core diam. mismatch	6.0	0	0
b)	Core N.A.	2.9	0	0
c)	Gap separation	0.6	0.6	0.6
d)	Axial misalignment	0	3.4	0.
e)	Angular misalignment	0	0	0
f)	P Fresnel reflection	.2	.2	.2
	Max. Total Loss	9.7	4.2	0.8

D. Optical power distribution at each connector (Minimum power launched into succeeding optical section)

a) Conn. No. 1 21.8 - 9.7 = 12.1 dbμw

Conn. No. 2 12.1 - 1.5 - 4.2 = 6.4 dbμw

Conn. No. 3 6.4 - 1.5 - .8 = **+ 4.1 dbμw**

(into detector)

E. Current Output from Photo Diode

P_{Min} · Res = 2.57 μw (.3 μa/μw) - **.77 μ amps**

Appendix 3

Optical Loss Calculations

(Theory vs. Experimental)

	Theory (max)	Exp. max/avg.
Splice No. 1 (emitter to size cable)	9.7 db	8.8/8.3 db
Splice No. 2 (size to size cable)	4.2	7.6/3.0
Splice No. 3 (size to detector)	0.8	1.2/.45
Size cable attenuation (50m)	1.5 db	2.5/1.9
Transmitter output power (I_f = 100 ma)	150 μw (min)	148 μw (min)
Receiver responsivity	.30 (avg)	.32/.30

Notes:

1 Due to instrumentation available this value may vary by ±25 percent.

Appendix 4

Optical Receiver Noise Measurement:

Meter: Hp 3400A RMS Voltmeter

a) Zm = 600

b) f_{3db} = 10 mhz

Accessories: Interstage amplifier, A = 10

a) R_L = 2.15 kΩ

System layout:

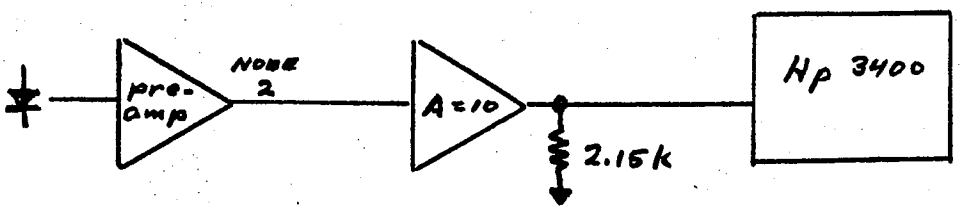

P_n (measured) = -60 dbmw into 2.15 kΩ load

$$P_n(\text{corrected}) = 20 \log \left(\frac{7.75 \times 10^{-4}}{.775} \right) + 10 \text{ Log } \left(\frac{600}{2.15k} \right)$$

$$= -60 \text{ db} - 5.54 \text{ db}$$

$$= -75.5 \text{ dbmw}$$

V_{OUT} (R_L = 2.15k) = 7.8×10^{-4} Volts

V_{OUT} (-20 db) = 7.8×10^{-5} Volts - subtract x 10 from interstage amplifier

$$\text{InRms} = \frac{7.8 \times 10^{-5}\ V}{10K}$$

$$= \boxed{7.8\ n_a} \quad \text{into front end of amplifier}$$

Appendix 5

A. Bit error rate (BER) noise measurement:

P_{in} (launched into pigtail) = -4.0 dbμw

P_D (power delivered to diode) = -4.0 - .45 db

= -4.45 dbμw

= .359 μw

I_s (rms signal current) = .359 μw (.3A/w)

= .108 μa

i_n (rms noise ~ -11 db below signal current) = .108 μa (.28)

= 30.2 na

NOTES:

1 BER = 4.0×10^{-3} for 11 db signal to noise ratio. This assumes an rms gaussian noise characteristic for a random 2-level polar transmission.

B. System signal to noise calculation

P_n (noise power R_L = 5.11k) = -36.5 dbmw

$$P_n \text{ (corrected)} = 20 \text{ Log } \left(\frac{.0115}{.775} \right) + 10 \text{ log } \left(\frac{600}{5.1k} \right)$$

= -36.6 - 9.3

= -45.9 dbmw

V_n (max output signal) = 25.2 dbmw

S/N = 45.9 + 25.2 = 71.1 db

Appendix 6

Distortion Measurements

Total harmonic distortion:

$$T.H.D. = ((A_1)^2 + (A_2)^2)^{1/2} \times 100$$

$$A_1 = 10^{-55/20}$$

$$= .0018$$

$$A_2 = 10^{-60/20}$$

$$= .001$$

$$T.H.D. = ((.0018)^2 + (.001)^2)^{1/2} \times 100$$

$$= \boxed{.21 \text{ percent}}$$

$$I.M. = ((.0018)^2 + (.0056)^2 + (.0032)^2)^{1/2} \times 100$$

$$= \boxed{.67 \text{ percent}}$$